RSC Advances

REVIEW

View Article Online
View Journal | View Issue

Cite this: *RSC Adv.*, 2024, **14**, 13413

Recent advances in the functionalization, substitutional doping and applications of graphene/graphene composite nanomaterials

Jyoti Narayan * and Kangkana Bezborah

Recently, graphene and graphene-based nanomaterials have emerged as advanced carbon functional materials with specialized unique electronic, optical, mechanical, and chemical properties. These properties have made graphene an exceptional material for a wide range of promising applications in biological and non-biological fields. The present review illustrates the structural modifications of pristine graphene resulting in a wide variety of derivatives. The significance of substitutional doping with alkali-metals, alkaline earth metals, and III–VII group elements apart from the transition metals of the periodic table is discussed. The paper reviews various chemical and physical preparation routes of graphene, its derivatives and graphene-based nanocomposites at room and elevated temperatures in various solvents. The difficulty in dispersing it in water and organic solvents make it essential to functionalize graphene and its derivatives. Recent trends and advances are discussed at length. Controlled reduction reactions in the presence of various dopants leading to nanocomposites along with suitable surfactants essential to enhance its potential applications in the semiconductor industry and biological fields are discussed in detail.

Received 17th October 2023
Accepted 1st April 2024

DOI: 10.1039/d3ra07072g

rsc.li/rsc-advances

1 Introduction

Recently, graphene (Gr) and graphene-based nanomaterials (GNMs) have gained the attention of the scientific world as some of the most promising carbon nanomaterials. Two profound scientists, Andre Geim and Konstantin Novoselov,[1] successfully separated graphene from graphite in 2004.[1] Its unique physico-chemical properties, such as large specific surface area, mobility, chemical stability, easy modification with different functional groups, better resultant solubility, excellent thermal and electrical conductivities, simple methods of preparation, effortless encapsulation and recyclability, have made it a subject of curiosity in the domain of nanoscience and nanotechnology. Due to specialties within Gr/GNMs, they reveal potential applications ranging from high-speed radio frequency logic devices[2] to thermally and electrically reinforced composites, photocatalysis[3,4] solar cells[5,6] sensors[7–9] and transparent electrodes especially for liquid crystal displays,[10,11] besides having quantum potential in the fields of biotechnology, biomedicine, bioengineering, and disease diagnosis and therapy. However, a systematic understanding pertaining to its physico-chemical properties and biochemical interactions is hardly available in the literature. It has been observed that graphene links with nanoparticles through hydrophobic, electrostatic, and covalent-bond interactions and synergistic effects, which prevent π–π stacking between graphitic sheets and thus aggregation between the nanoparticles. A lot of work is still needed to investigate the reasons for and origin of these interactions between Gr/GNMs. This field has not yet been addressed and explored to a considerable extent; thus, it requires in-depth investigation and scientific understanding as a wide variety of derivatives of pristine graphene has recently been reported.

1.1 New carbon materials: derivatives of wonder graphene

Graphene and its derivatives are referred to as graphene-family nanomaterials.[12–16] Over the past five years[17–22] the skeleton chemical structures of graphene and its modifications have revealed a good number of new carbon nano-materials derived from graphene experimentally and theoretically. These are oxidized graphene (graphene oxide), hydrogenated graphene (graphane), fluorinated graphene (fluorographene), graphyne and graphdiyne, designated as graphene with introduced acetylenic chains. In case of the latter, it has been observed that the introduction of acetylenic or di-acetylenic chains between carbon hexagons results in a layer of single-atom thickness, which appears flat like graphene. Fig. 1 presents the chemical structures of graphite (a), graphene (b), graphyne (c), graphdiyne (d), fluorographene (e), graphene oxide (f), reduced graphene oxide (g) and graphone (h). The parallelogram drawn in Fig. 1(b–d) represents a unit cell. Various arrangements of acetylenic linkages, which lead to various derivatives of graphene, are reported in Fig. 2. The chemical structure of graphene is basically a flat monolayer of two-dimensional

Synthetic Nanochemistry Laboratory, Department of Basic Sciences & Social Sciences, (Chemistry Division) School of Technology, North Eastern Hill University, Shillong 793022, Meghalaya, India. E-mail: jnarayan.nehu@gmail.com

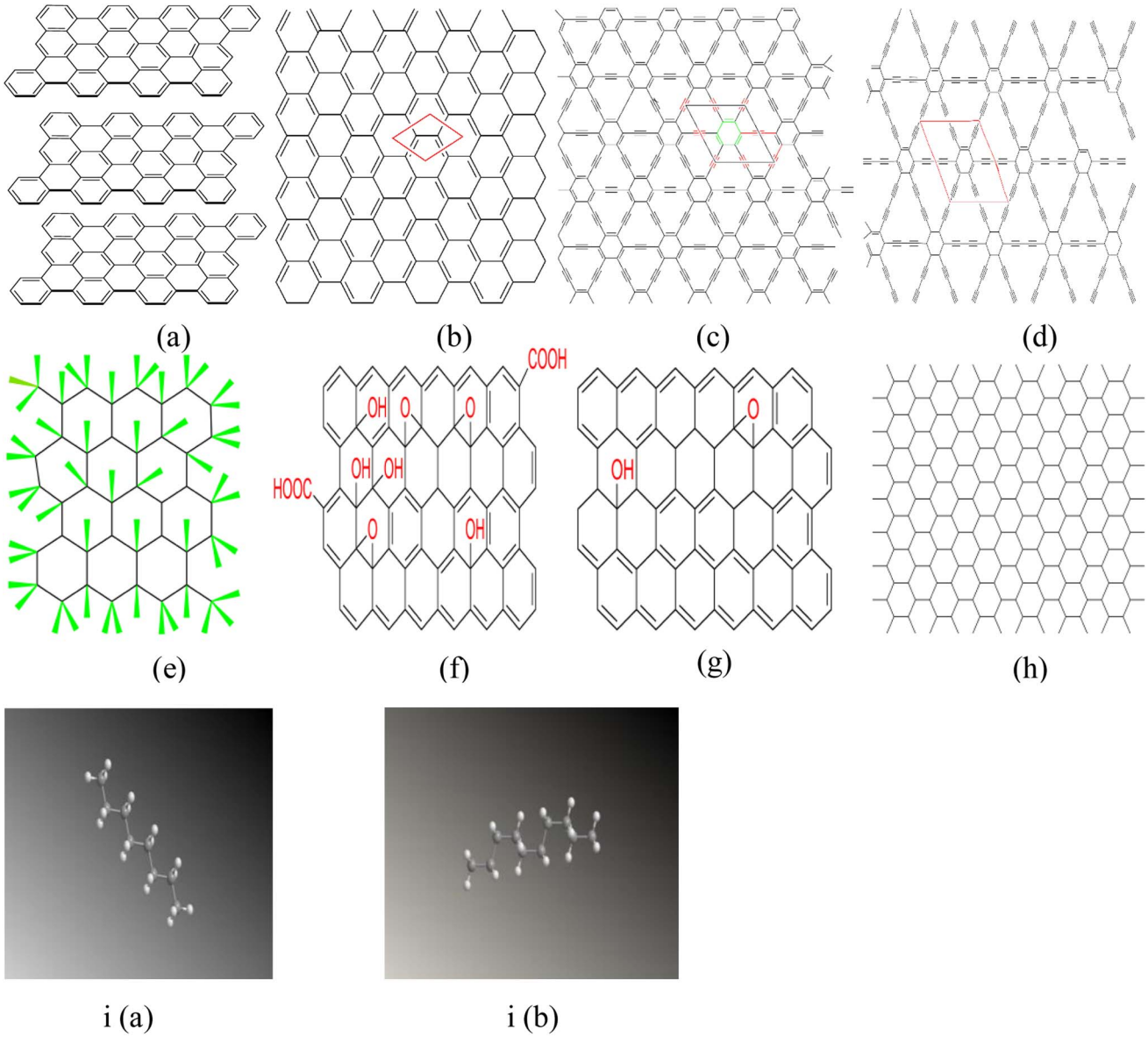

Fig. 1 General skeleton of the chemical structure of graphite (a), graphene (b) and its derivatives, graphyne (c), graphdiyne (d), fluorographene (e), graphene oxide (f), reduced graphene oxide, (g) graphone (h), chair and boat-like conformations of graphane i(a) and i(b). The parallelograms drawn in these illustrations represent a unit cell.

hexagonal carbonaceous honeycomb crystalline sheets with a single-atom thickness derived from crystalline graphite (Ganganboina and Doong, 2020).[15,16,23] It is composed of a layer of independent sp^2-hybridized carbon atoms, mixing s, p_x and p_y atomic orbitals. Each carbon in graphene is reported to be bonded to three adjacent carbon atoms through a σ bond. The π-electrons undergo π-bond formation with surrounding atoms due to being unbounded. The π-bond direction is found to be perpendicular to the graphene plane. The structure of graphene is highly stable, strongest and thinnest: the thickness observed is 0.34 nm, and the C–C bond length found is to be 0.142 nm,[14] and covalently bonded pure carbon atoms are interconnected by van der Waals forces in the same plane with differences in electrochemical characteristic between its edges and the basal plane. No rearrangement or realignment is observed when it is subjected to high pressures and forces except for the deformation observed in the atomic surface. Fig. 1(c) reveals the possibility of the formation of a flat single atomic layer by connecting the carbon hexagons by linear carbon chains. One-third of carbon–carbon bonds in graphene are replaced by the acetylenic linkages. This structure is called graphyne, which is made up of sp–sp^2 hybrid C-atoms with a 2D layered structure in plane porous geometries. This results in an unusual topological and electronic structure with high charge mobility, good electronic transport capabilities and acetylenic chains between neighboring benzene rings in each graphyne unit.[24] Conversely, graphdiyne (GDY) (Fig. 1(d)), a 2D periodic carbon allotrope, differs significantly from graphene hybridized orbitals (Fig. 1(b)), as the latter contain only single and double bonds.[25] GDY is formed due to the presence of two acetylenic (di-

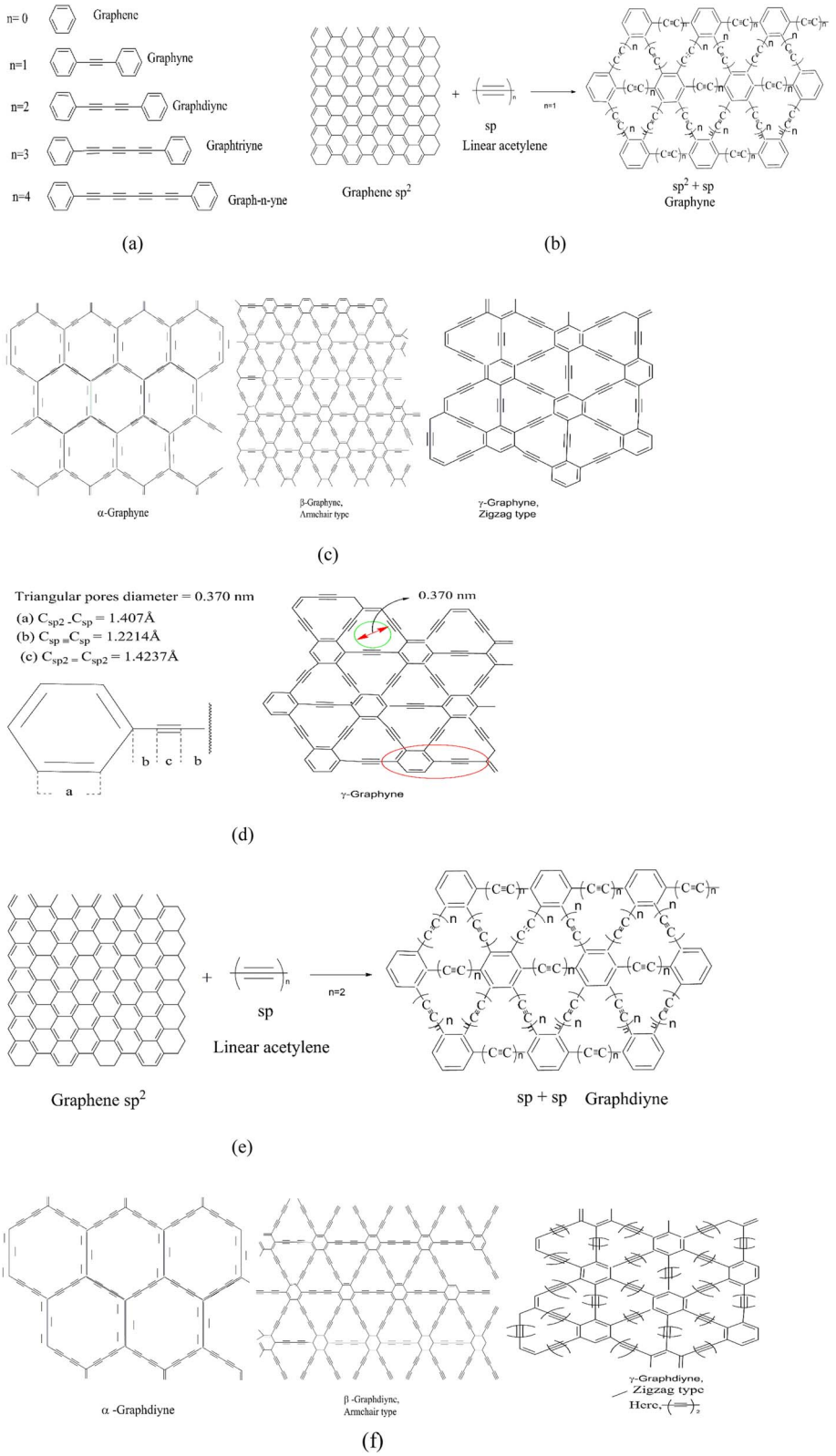

Fig. 2 (a) Number of linkages in between two hexagons ($n = 1$ to $n = 2$). (b) Formation of the schematic structure of graphyne (GY). (c) Different types of graphyne conformation. (d) Lattice parameter and triangular pores of graphyne. (e) Formation of the schematic structure of graphdiyne (GDY). (f) Types of graphdiyne.

acetylenic) linkages. The linear carbon chains between the carbon hexagons composed of the acetylenic linkages (–C≡C–) are more stable than cumulative linkages (=C=C=).[26] Various arrangements of patterns of the acetylenic linkages to form a flat atomic layer of carbon atoms have been reviewed theoretically[27,28] Fig. 2(a) presents the number of linkages between two hexagons ($n = 1$ to $n = 4$). Based on the number of ethyne units (n) between two sp^{2-} hybridized carbon atoms, graphene can be classified into different categories, such as graphyne (GY) (two adjacent sp^2-hybridized carbon atoms are connected by n "–C=C–" linkages), graphdiyne (GDY), graphtriyne (GTY), and graph-n-ynes (G_nY). Fig. 2(b) and (e) present the formation of schematic structural representations of GY and GDY as a result of linear acetylenic and di-acetylenic linkages to graphene.

Depending on the combinations of sp and sp^2-hybridized carbon atoms, three types of GY (α, β, and γ; Fig. 2(c)) and GDY (α, β, and γ; Fig. 2(f)) are proposed. Based on density functional theory calculations, Kim *et al.*[29] predicted that γ-GY exhibited a lattice parameter of $a = 0.686$ nm (2D hexagonal *p6m* symmetry) with a periodic distribution of triangular pores with a diameter of 0.370 nm (Fig. 2(d)). The optimized bond lengths of C_{sp^2}–C_{sp} ($a = 1.407$ Å), C_{sp}≡C_{sp} ($b = 1.2214$ Å) and $C_{sp^2} = C_{sp^2}$ ($c = 1.4276$ Å) were reported. A binding energy of 7.95 eV per atom was estimated for the γ-GY form, which was found to be almost the same as for graphite (8.87 eV per atom), indicating its high thermal stability.[27] Conversely, a binding energy value of 7.78 eV per atom and the lattice parameter of $a = 0.944$ nm have been recorded for graphdiyne.[14] Graphyne and graphdiyne are semi-conductive materials with band gaps of about 0.5–0.6 eV. They have considerably small effective masses for carriers.[26] One can comparatively study the structure and properties of graphyne and graphdiyne with that of graphene, but they cannot be prepared directly from it. Fig. 1(e) shows a 2D stoichiometric graphene derivative called fluorographene (FG). The electrical and optical characteristics of fluorinated graphenes are significantly affected by the ratio of fluorine (F) atoms inserted into the carbon lattice (C/F, sp^2/sp^3).[30] It has been observed that even a small amount of fluorine atoms in the graphene structure can give rise to band opening and adsorption spectra, exhibiting its transparency in the range of visible light.[31] The spectrum shows that FG starts the absorption of light in the blue region (energy > 3.0 eV) indicating that FG is a wide-gap semiconductor or an insulator with a wide band gap of ≥3.0 eV. J. T. Robinson *et al.*[32] reported that various systematic studies of several single-sided periodic arrangements of fluorine atoms on graphene, for a number of different coverages, have been taken up. They reported that the introduction of fluorine to graphene modifies the electronic properties of graphene by reducing the charge in conducting π-orbitals (i) by introducing scattering centers and (ii) by opening the band gaps. These effects have been found to be consistent with the reduction in conductivity and mobility. It was observed that with increasing F coverage, the band gap widens, and the Fermi level is lowered in the valence band. These effects occur due to the interaction of the p-orbital of F with the π-orbital of carbon producing sp^3 bonds, which results in the modification of charge densities and introduces scattering centers for conduction. C_4F specifically showed a band gap of 2.93 eV leading to optical transparency. π bands are largely disrupted, giving rise to π resonances surrounded by sp^3-bonded C atoms. Low-ordered coverage of F can also open an appropriate band gap in graphene. Thus, single-site fluorination of graphene can also considerably modify the transport properties of graphene-based materials and thereby can have potential applications in the device-making domain. Graphene oxide (GO) (Fig. 1(f)) is an incredible physico-chemical material with a small size, large surface area and exceptional strength in a 2D structure. Hydrophilicity is an excellent property of GO particles, resulting in a wide range of concentrations. They produce stable aqueous dispersions. Reduced graphene oxide (rGO; Fig. 1(g)), is a captivating member of the graphene family as it is the only type along with GO that can be scaled up and made on a kg scale.[33–35] A chemical and thermal process is used to reduce the quantity of oxygen in the material as it makes GO more unstable. Fig. 1(h) reveals the structure of graphone. It is a half-hydrogenated graphene (a graphene sheet with 50% hydrogenation and stoichiometric C_2H). The structure of graphone is displayed as trigonal adsorption of hydrogen-atoms on graphene. H-atoms are only on one side of carbon sheets, resulting in a mixture of hybridized sp^2 and sp^3 C-atoms. Upon geometric relaxation, it was found that graphone has some zigzag shape.[36,37] It has been examined in a number of studies that investigated band gap modulation, ferromagnetism, antiferromagnetism, spin–orbit coupling, and structural and thermal stability.[38] Fig. 1(ia) and (ib) reveal a fully hydrogenated derivative of graphene, with chemical composition CH, called graphane. It processes sp^3 C–C bonds and consequently has a carbon-atom layer which is puckered. The literature reveals interesting properties for graphane and partially hydrogenated graphene.[39] It is predicted theoretically that thermal energy in the case of graphane is well accommodated by in-plane bending modes, usually C–C–C bond angles in the puckered carbon layer, whereas in the case of graphene, it is out-of-plane fluctuation modes. The thermal properties of graphane (up to 1500 K) and molar heat capacity (29.32 J mol^{-1} K^{-1}) were found to be a bit larger than those of graphene.[40,41] Theoretically, it is predicted that there will be a gradual increase in the band gap from 0 eV for graphene to 4.4 eV for graphane.[42] Conversion of graphene to fully hydrogenated graphane predicted a change in magnetic and electronic properties, thus exhibiting the potential ability to convert metals to semiconductors and non-magnetic materials to magnetic materials, respectively.[36] The overall flowchart of various possible structural conversions from graphene to its other derivatives is reported in Fig. 3.

2 Substitutional doping of graphene and its significance

The literature reveals that chemical doping is a promising approach for achieving effective and high-efficiency graphene nano-films with a larger carrier concentration as a result of an

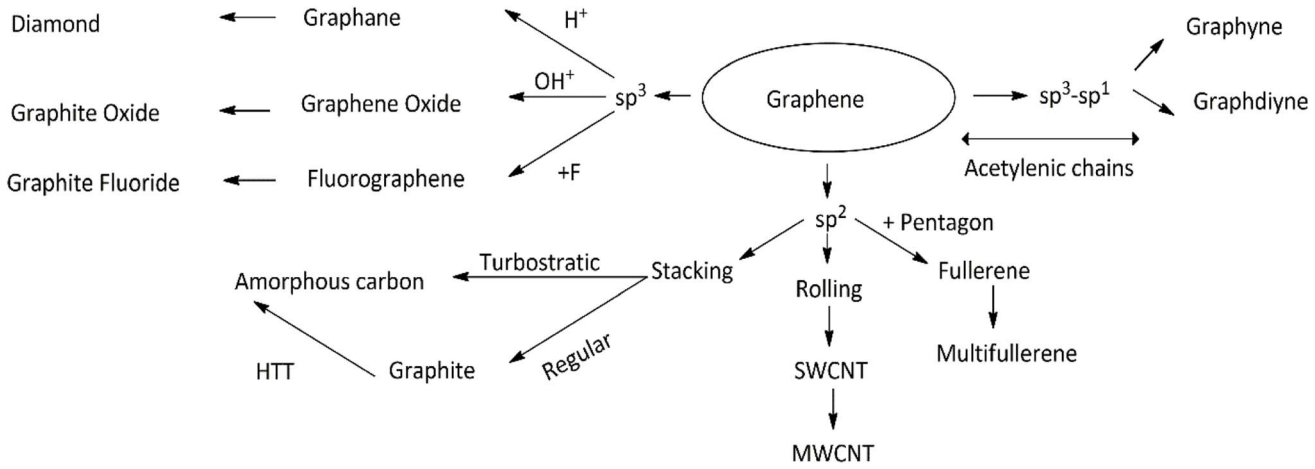

Fig. 3 Representation of the overall flowchart of various possible structural conversions from graphene to other derivatives.

alteration in the electronic properties. Substitutional doping of graphene with non-magnetic elements such as N or B can be achieved effectively during the growth process of graphene.[43–46] Zhao *et al.*[43] revealed that substitutional doping in monolayer graphene during growth can be used to alter its electronic properties. Single nitrogen atoms can be incorporated as graphitic dopants, and a fragment of the extra electron in each hydrogen atom can be delocalized into the graphene lattice. This has resulted in enhanced modifications in a few specific sites of the nitrogen dopant within the structure of nitrogen-doped graphene nanomaterials. Terrones *et al.*[44] emphasized the importance of defective graphene or graphene-like materials. At the bulk level, these defects result in a drastic degradation in performance, but at the nanoscale, they are extremely helpful for generating novel and promising nanomaterials such as (2D) graphene and (1D) graphene nano-ribbons. Apart from structural sp^2-like defects, they also discussed topological sp^2-like and sp^3-like defects, vacancy/edge type defects (non-sp^2-like), doping or functionalization sp^2 and sp^3. These defects could critically affect the physico-chemical properties that could be helpful in the engineering of new nanoscale materials in the future. There has hardly any work in this domain been done so far. Peralta *et al.*[45] analyzed the electronic and transport properties of graphene with lithium (Li) and potassium (K) alkali adatoms. The two alkali metals are of great technological interest. They have potential applications in energy storage and superconductivity. Both adatoms facilitate studies on the dynamics of graphene quasi-particles and thereby minimize conductivity. Two inequivalent metal adsorption sites, namely, the top site (T) which is on the top of the carbon atom of one sub-lattice of graphene and the hollow site (H), that is in the middle of the C_6 unit, were studied. An analytical tight-binding Hamiltonian model was used to analyze two sites of adsorbate atoms in graphene. In contrast, they used the Green's function equation of motion to calculate the corresponding band structures and density of sites in addition to numerical calculations of conductance with a Python quantum transport simulation model. It was observed that the bands are downshifted with respect to pristine graphene, which indicates doping with electrons. For the top case, the AB symmetry breaks, generating small band gaps of around 170 meV for potassium and 220 meV for lithium. Scardamaglia *et al.*[46] reported the vertical distribution of alkali ion (Na, K, and Cs) distribution on multi-layered graphene generated on SiO_2 in vacuum and in the presence of water vapour, using standing wave ambient pressure photoemission spectroscopy. It was found to be different from hard graphite. They concluded that Cs, K, and Na ions do not intercalate into multi-layered graphene under vacuum conditions, which was attributed to the reversibility of the process, due to large inter-sheet spacing or lack of time for intercalation. In contrast, when exposed to water vapour, Na ions intercalate in soft carbon, whereas Cs ions do not. This was a clear indication of the difference in the intercalation mechanisms on hard graphite and soft graphene. In fact, intercalation of electron-donating species often leads to the opening of a band gap at the Dirac point, a change in the spin–orbit coupling in graphene induced by intercalated species[47] or a shift in the Fermi level upwards to the van Hove point.[48] Careful control over the intercalation process makes it possible to construct a p–n junction[49] or to form ferromagnetic islands.[50] Recently, experiments have shown that single- and few-layered graphene sheets can be turned into superconductors by doping with Li,[51] K,[52] or Ca.[53] Currently, it is a well-known fact that nanoscale nonlinear optical (NLO) materials have gained huge attention from scientists in recent decades because of their enormous applications in optics, electronics, and telecommunications. Carbon-based nanoscale materials are one of the most important classes of NLO materials; they have highly delocalized π-electrons, which are responsible for their NLO response.[54,55] Such materials with exceptionally high values of hyperpolarizability have been developed by doping or structurally modifying graphene, with a two-dimensional (2D), sp^2-hybridized allotrope of carbon.[56] A novel way of making NLO materials has been put forward by Sarwar *et al.*[57] They employed density functional theory (DFT) calculations, which helped them to explore the effect of alkali metal (Li, Na, and K) doping on the nonlinear optical response of tetragonal graphene quantum dots (TGQDs). Sarwar *et al.*[57] reported that hardly any study has been

made of the role of the alkali metal (Li, Na, and K) doping leading to the triggering of non-linear optical response of nanomaterials by converting their centrosymmetric configuration into a non-centrosymmetric configuration. They theoretically proposed four stable geometries for each Li-doped TGQD and three for each Na- and K-doped TGQD. They evaluated several physico-chemical properties to show the impact of the alkali metals. The interaction distance ($D_{int.}$, Å) of the alkali metal (Li, Na, and K) in respective geometries indicated that the interaction distance between TGQDs, and the alkali metals showed an increase, as the atomic number of the considered alkali metal increased. Since thermodynamic stability is an important criterion for the synthetic usefulness of NLO materials, binding energies, charge transfer (among alkali metal and TGQDs) and dipole moment, revealing the polarity of the TGQDs, were calculated. Amongst these properties, the binding energies described the stability of doped complexes (TGQDs: Li@rp, Li@r8d, Li@r8a,Li@rc, Na@rp, Na@r8d, Na@@r8a, K@r8d, K@r8a and K@rc). A greater binding energy value represented better interaction between two components (M@TGQDs); as a result, greater thermal stability of the doped complexes was observed. The binding energy values of Li-doped TGQD isomers was found to be larger than those of the corresponding Na- and K-doped TGQD isomers: the values for Li@r8d, Na@r8d, and K@r8d are −45.58, −30.92, and −39.50 kcal mol^{-1}, respectively.[57] Similarly, Li@r8a, Na@r8a, and K@r8a showed binding energies of −43.58, −30.05, and −38.83 kcal mol^{-1}, respectively. In the case of M@rc isomers, binding energy values were found to be −36.42, −24.58, and −36.12 kcal mol^{-1} for Li@rc, Na@rc, and K@rc, respectively. From these values, it can be concluded that Li@r8d was the most stable among all the complexes.[57] Selected alkali-metal-doped TGQD complexes showed reasonably high negative values of the binding energies, indicating the feasibility of the doping process. In general, all these theoretically designed alkali-metal-doped TGQD complexes possessed good thermodynamic stability. The natural bonding orbital (NBO) charges on the alkali metals were observed in the range 0.940–0.984 e^{+}, which implied sufficient ability to shift charge from the alkali metals to the TGQDs. Charge transfer has a direct relationship with NLO properties.[58] Thus, this charge transfer would induce large dipole moments and polarizabilities, which in turn would aid in the improvement of the NLO properties. The dipole moment is another parameter that reveals the polarity of the system. It is a tool to determine the charge separation in the system. As the charge separation between negative and positive charges increases, the polarity of the system rises, and as a result, the dipole moment of the system also rises. The dipole moment of the undoped TGQDs is 0.013 D. Alkali metal doping resulted in a significant increase in the dipole moment of the TGQDs. For instance, the dipole moments of Li@r8d, Na@r8d, and K@r8d were 4.67, 6.97, and 8.93 D, respectively. As the dipole moment is dependent on the extent of the charges and distance between them, a high value of charge on the K atom in the K@r8d complex was reported to be responsible for its large dipole moment. Overall, an increase in the dipole moment was found after doping the TGQDs with the alkali metals, which is helpful in inducing adequate polarizability and hence an improved NLO response. From the molecular electrostatic potential (MEP) analysis, designation of the charge distribution of a system can also be studied. MEP is very helpful in linking the molecular structure to the physical and chemical properties of the complexes. These properties include chemical reactivity, partial charges, and the dipole moment.[59,60] With reference to MEP mapping, red and yellow colors indicate negative charge. Therefore, areas showing red and yellow colors are predicted to be electron-rich regions. However, the alkali-metal-doped TGQD complexes showed a blue color, indicating the regions that are electron deficient and exhibited a positive charge. This positive charge was found because of the shifting of valence electrons of the alkali metal to the TGQDs. This transfer of electrons thus created diffused excess electrons. The areas with a green color indicate the mean potential, and hence green areas are predicted to be neutral.[59] The size of the blue area increased with the increasing size of the alkali metals, which indicated more efficient charge transfer between the alkali metals and TGQDs. However, the TGQD complexes showed a uniform charge distribution. Thus, MEP analysis confirmed that the designed complex M@TGQDs contains a significant charge distribution of electrons, resulting in prominent variation in their dipole moments, which was found to be important for the NLO response. Besides the molecular electrostatic potential study, global reactivity descriptors for ionization potential, electron affinity, chemical hardness and softness and the chemical potential of graphene materials under discussion were also helpful for predicting the impact of doping with different alkali metals on the nonlinear optical response of the TGQDs. The global reactivity descriptors are linked with the NLO response of the materials; for example, a complex with smaller ionization potential values exhibits a high NLO response. Similarly, an enhanced NLO response is expected from the complexes with higher softness or lower hardness values. It is also known that HOMO and LUMO energies are directly linked with ionization potential and electron affinity, respectively. The negative of the HOMO energy is almost equal to the ionization potential and that of the LUMO energy is almost equal to the electron affinity (Koopmans approximation)[61] According to Sarwar *et al.*,[57] undoped TGQDs showed an ionization potential of 4.89 eV, and the electron affinity value was 3.24 eV. Doping of alkali metal into the TGQDs showed decreasing data for ionization potential and electron affinity. The ionization potential values were 4.19 eV for Li@rp, 4.22 eV for Li@r8d, 4.33 eV for Li@r8a, and 4.08 eV for Li@rc complexes. This decreasing trend in values of ionization potential for the doped TGQD complexes indicated the ease of ionization to generate diffuse excess electrons and hence improved NLO response values. Similarly, the electron affinity, which is related to the ability of a system to gain an electron, is also modified after doping with the alkali metal atom. For example, the electron affinity ranged from 2.62 to 2.80 eV for Li@TGQDs, from 2.47 to 2.60 eV for Na@TGQDs, and from 2.36 to 2.50 eV for K@TGQDs complexes. The electron affinity of the undoped TGQDs was found to be 3.22 eV. The chemical hardness of the M@TGQDs has also been found to be linked to the

stability of a system,[59] and its value was found to be 0.82 eV for undoped TGQDs, which is greater than the values for M@TGQD complexes, indicating that undoped TGQDs are more stable and less reactive and hence exhibit a smaller NLO response than doped complexes. Conversely, the chemical softness value is directly related to the NLO response; thus, an increase in softness is usually linked with an increase in the NLO response.[62] The chemical softness of pure TGQD was 0.61 eV, which increased after doping, and the maximum chemical softness among the doped complexes was 0.78 eV for Li@rc. The chemical potential value was found to be −4.07 eV for the undoped TGQDs, which decreased monotonically from Li- to K-doped complexes. The chemical potential was −3.41 eV for Li@rp, whereas it was −3.49 eV for Li@r8a, −3.31 eV for Na@r8a, and −3.19 eV for K@r8a. A similar trend in chemical potential was observed for M@r8d and M@rc (M = Li, Na, K) complexes. The chemical potential values of the M@TGQD complexes were found to be less than those of the undoped TGQDs, indicating that the designed complexes are less stable and more reactive, which leads to an enhanced NLO response.[63] The NLO properties of a system can be improved to a greater extent by introducing excess electrons into the system. These excess electrons generate new HOMO orbitals, which are higher in energy, and as a result, the HOMO–LUMO gap is decreased. These excess electrons also result in increasing polarizability and first-order hyperpolarizability values of the system. For the undoped TGQDs, the calculated polarizability was 420 au. The alkali-metal-decorated TGQD complexes showed enhanced polarizability values. The K-atom-doped TGQD complexes exhibited relatively better polarizabilities. The highest polarizability was computed to be 476 au for K@r8a isomers. K@r8d and K@rc showed polarizabilities of 475 and 474 au, respectively. Theoretically calculated polarizabilities for Na@r8d, Na@r8a, and Na@rc isomers were reported to be 470, 471, and 471 au, respectively. Li@TGQDs complexes showed comparatively lower polarizabilities of 470, 465, 467, and 470 au for isomers like Li@rp, Li@r8d, Li@r8a, and Li@rc, respectively. Comparison of the hyperpolarizabilities of the alkali-metal-doped TGQDs complexes revealed that the highest hyperpolarizability value exhibited by Li@r8a was 5.2×10^5 au, for Na@r8a was 3.7×10^4 au, and K@r8a revealed 2.74×10^4 au. The Li@r8a isomer showed a greater NLO response than all above-mentioned compounds, which suggests it is a more efficient NLO material for optics and optoelectronics applications. The NLO response of graphene quantum dots (GQDs) has also been investigated, showing that changing the shape, size, and edge modifications with different atomic species causes a very prominent change in the NLO response. Sharma *et al.*[64] reported the tunability *via* size, shape and relatively low level of loss and high level of spatial confinement in the graphene quantum dots (GQDs) resulting in effective excitation in the GQDs, showing high energy plasmon frequency along with frequencies in their terahertz (THz) region, making them a powerful material for photonic technologies. Their studies have reported a systematic investigation of linear and non-linear optical properties of various types of GQDs in size and topology using the advantages of semiempirical as well as first-principles methods. Among the circular, triangular, random and stripe-shaped GQDs, they found that the GQDs with inequivalent sublattice atoms always possess a lower HOMO–LUMO gap, broadband absorption and a high non-linear optical coefficient. The majority of these GQDs with linear and non-linear properties revealed zigzag edges.[64,65] The reported GQDs have a near linear dependence on the number of edge atoms and a HOMO–LUMO gap with a particular number of carbon atoms that can be tuned from 0 to 3 eV depending on its size and edge nature. Marchiani *et al.*[66] reported electron doping with potassium alone on free-standing nanoporous graphene. This avoids any influence of the substrate on the metallicity of the material. The tracked electron transport in the π-antibonding downward-shifted conduction band. The rigid band shift and spectral density of the π-antibonding state in the upper Dirac cone with the associated plasmon, showed a blue shift with increasing dose of potassium ions. This was observed from deduced electron energy loss spectroscopy. Spatially resolved photoemission confirmed the Dirac plasmon activated by C 1s emitted electrons. A significant correlation between electronic π-antibonding states in the conduction band, and the Dirac plasmon evolution upon *in situ* electron doping of fully free-standing graphene was established.

Surface charge transfer doping (SCTD) is an emerging doping technique that is able to provide an effective and non-destructive doping capability on 2D semiconductors.[67] SCTD depends on the interfacial charge transfer between surface dopants and the host semiconductor without producing notable defects in the 2D crystal during the doping process. Owing to the extremely large surface to volume ratio, the doping level inside 2D semiconductors is dominated by the degree of charge transfer occurring at the surface, indicating the strong doping capability of SCTD. It features simple coating of dopants on the 2D surface without sophisticated device formation or energy consumption. Thus, it is widely used to dope not only 2D semiconductors but is also used to tune their electrical and optical properties that facilitate the rational design and construction of 2D-based functional devices with optimized performance. Ma *et al.*[68] reported that surface charge transfer doping is an important strategy for the modulation of the electrical and optical properties of graphene. They said that, in contrast to other doping methodologies, surface charge transfer doping exhibits distinct advantages in various aspects like minimized negative impact on the carrier mobility without disrupting the graphene lattice, wide range and precise control over the doping concentration and highly efficient treatment processes without using high temperature or ion implantation. Thus, efforts are being made to develop diverse surface charge transfer p- and n-type dopants, which include alkali metals, alkaline metals, transition metal acids, gases, metal chlorides, metal oxides, organics containing electron-donating/withdrawing groups, ferroelectric organics, and carbon-based materials, that could serve as a wide range of pathways to modulate the properties of graphene. Recently, remarkable progress has been made in realizing heavy and stable doping by surface charge transfer. The literature reveals that, if boron, nitrogen, phosphorous and aluminium atoms are substituted

for carbon atoms in graphane, conversion from a semiconductor to a metal can take place. About 3.2–3.8 mass% enhancements in hydrogen storage capacity have been observed when graphene has been doped by lithium. Recently, the idea that hydrogen molecules (H_2) as a clean energy carrier that can replace fossil fuels in the future is gaining momentum. It can mitigate rapidly growing demands for energy and thus slow down global-climate changes in the future. The only challenge is its storage. Thus, the concept of materials-based storage is coming to the fore in a huge way. The urge to design and prepare such materials has been explored quite extensively in recent years. A potential H_2 storage material should be able to store a sufficient amount of hydrogen at ambient pressure and temperature. This requires the storage material to have a large surface area and low molecular weight and suitable interaction between hydrogen molecules and host material, which should lie between weak physisorption and strong chemisorption. The H_2 adsorption energy should lie in the range of 0.1–0.2 eV/H_2 for an ideal hydrogen storage system.[69] Carbon-based nanomaterials are considered favorable to meet these criteria. Hussain *et al.*[70] predicted (from first-principles density functional calculations) that pre-hydrogenated, Li-doped graphane, LiCH, could be a potential candidate for hydrogen storage. Their study showed that the calculated Li-binding energy on graphane is significantly higher than the cohesive energy of Li bulk, thus ruling out any possibility of cluster formation in Li-doped graphane. They revealed that, even with a very low concentration (5.56%) of Li doping, the Li-graphane sheet achieved a good hydrogen storage capacity of 3.23 wt%. They calculated hydrogen adsorption energies in the desired range of 0.1–0.2 eV, suitable for achieving H_2 storage at the operating temperature and pressure conditions in mobile applications. The lithium binding energy in the LiCH sheet was found to be 2.94 eV, which was reported to be much greater than the cohesive energy of Li bulk (1.6 eV), ruling out the possibility of cluster formation in Li-doped graphene. Similar work was also reported by Khazaei *et al.*[71] Using first-principles electronic structure calculations, they studied the stability, electronic structure and hydrogen storage capacity of two newly designed mono-layered LiCH and LiBNH nanomaterials. The hydrogen atoms on one of the faces of a graphane sheet which was pre-hydrogenated graphene, was substituted with Li atoms. The resulting monolayer was observed to attain a good hydrogen storage capacity of around 3.8 wt%, close to the revised Department of Energy DOE target. Within the chemical structure of the monolayer, lithium atoms are strongly hybridized and donate their electrons to the substrate, and as a result, their bonding energy to the surface attains a value of 3.27 eV, which is larger than the cohesive energy of lithium in its metallic bulk structure. The result was attributed to the non-aggregation or reduced clusterization of the lithium atoms on the monolayer, particularly at high temperature and high doping concentration. Thus, carbon-based materials have established their capability for storing hydrogen.[72–77] However, extensive work in this direction is still warranted. A systematic and thorough density functional theory (DFT) study on the interaction of the elements in the first two groups of the periodic table with a graphane (hydrogenated graphene) sheet was attempted by Hussain *et al.*[78] They proposed using the generalized gradient approximation (GGA) to study the binding configuration, bond length, and charge transfer and band gap of each of the adatom systems in depth. Different doping concentrations varying from 3.125% to 50% were considered to gain a better understanding of the adatoms–CH interaction. They reported a certain trend in binding strength, bond length and charge transfer in the case of both alkali metal and alkaline-earth metal adatoms. Alkali-metal adatoms at a low doping concentration of 3.125% exhibited semiconductor behavior, whereas when doped at higher than the considered concentration, the product showed metallic behavior. In contrast, alkaline-earth metal-doped CH exhibited metallic behavior at all doping concentrations. Substitutional doping with magnetic elements (transition elements) is thermodynamically unfavorable, probably, due to their differential chemical structure. However, it has been achieved under non-equilibrium conditions. First, vacancies are formed by bombardment with electrons or ions, and subsequently, magnetic dopant atoms are deposited, filling the vacancies that have not dynamically annealed between the two steps. Such dual-step processes are difficult to control, especially given the complex dynamics of vacancies in graphene, strongly limiting their reliability, reproducibility, and scalability. Ultralow-energy (ULE) ion implantation has the potential to overcome these limitations and has been successfully applied to the substitutional doping of graphene with N and B and P and Ge. Since graphene, apart from its direct fermions as carriers, exhibits a long spin lifetime and diffusion length, it has been promoted as an excellent material for ultra-thin memory devices.[79] To enhance the magnetic functionality, flexibility, reproducibility, and scalability inherent to ion implantation, graphene has been doped to a limited extent with manganese (Mn) atoms (with a high magnetic moment among 3d transition metals) in a single carbon vacancy.[80] Mn retained the Dirac-like behavior of pristine graphene.[81] Substitutional doping offers high stability attributed to the excellent covalent bonding between the dopant atoms and surrounding carbon atoms in graphene, indicating the versatile behaviour of graphene that can be exploited in various fields of the semiconductor industry. However, the synthesis of quality graphene is essential so that it can be used as a smart baseline material for the fabrication of stable GNMs. The literature reveals[82] that, because of the small difference in electronegativity between C and H, C–H is essentially non-polar and thus non-reactive. This has largely limited the application of graphene materials. The formation energy of a metal atom on the graphene surface increases with an increase in metal coverage. Mostly, the structures of absorbed metals are at the bridged site for single metal atom absorption and results often in dimerized, linear, chain types or 3D tetrahedral clusters. As more and more metal atoms are absorbed on the graphene surface, strong interactions are generated that culminate in cluster formation. Within these clusters (solid materials), the cohesive energy consequently increases, leading to the separation of the constituent atoms apart to convert them to an assembly of neutral free metal atoms on the surface Thus, doping of graphene with metallic atoms is difficult to

demonstrate experimentally. This may be attributed to the binding energy between metal dopants and graphene being much lower than their cohesive energy, leading to the formation of clusters instead of uniform doping on the graphene surface. Lee *et al.*[83] further reported that large-sized metal atoms can create larger local curvature, favoring the chemisorption of small molecules (H_2O, O_2, and NO) from the ambient, thereby greatly limiting the practical application of such doped graphene derivatives. They reported the effect of gas adsorption on the change in magnetic properties of a platinum-doped graphene (Pt-graphene) system using first-principles density functional theory (DFT). They observed the induction of different magnetic properties due to four chemisorbed gas molecules (N_2, O_2, NO_2, SO_2) on Pt. No spin polarization with N_2 adsorption, local polarization with O_2 adsorption and complete polarization with NO_2 and SO_2 adsorption were revealed. Interestingly, a difference was found in the spin direction of gases and Pt-graphene. NO_2 adsorption induced the same spin direction on the substrate, while SO_2 induced the opposite spin direction. These differences in the magnetic properties of Pt-graphene against the type of gas molecules adsorbed are expected to play an important role in the application of these nanomaterials as gas sensors or spintronic devices. Dai *et al.*[84] reported the adsorption of gas molecules (NO, NO_2, and SO_2) over boron-, nitrogen-, aluminium- and sulfur-doped graphene using density functional theory. B- and N-doped graphene retained a planar form, while Al and S atoms protruded out of the graphene layer. Investigation revealed that NO and NO_2 bonded to B-doped graphene, while only NO_2 bonded to S-doped graphene. Al-doped graphene was much more reactive and bound to all gases, including O_2. According to their investigations, Dai *et al.*[84] suggested that B- and S-doped graphene could be good sensors for polluting gases (NO and NO_2). Ao *et al.*[85] using DFT reported the theoretical enhancement of CO adsorption through Al doping into graphene. Strong chemisorption of CO molecules was observed due to the formation of an Al–CO bond, where CO onto intrinsic graphene showed weak physisorption. Enhancement was determined by the large change in electrical conductivity after adsorption, where CO adsorption led to an increase in electrical conductivity *via* introducing a large amount of shallow acceptor states, suggesting a newly developed Al-doped graphene that would be an excellent candidate for gaseous chemi-nanosensors. Extensive studies on the subject are warranted due to the inconsistency of findings that have been reported so far. Amongst the IV–VII group element doped graphene/graphene derivatives, silicon (Si: $3s^2 3p^2$)-doped graphene (SiG) has been investigated less than nitrogen or boron. Its chemistry reveals that silicon would obtrude out of the plane in the SiG structure as Si–C has a larger bond length (1.76 Å) than the C–C bond (1.41 Å). Deviation from a perfectly flat sp^2-hybridized carbon layer would theoretically result in SiG composites.[86] Y. Zou *et al.* (2011) and Y. Chen *et al.* (2013) reported the increased chemical reactivity of SiG owing to the structural change bought about by Si dopants. *Ab initio* calculations in DFT indicated that Si incorporated in graphene results in an increase in adsorption energy, for probing gas molecules like CO, O_2 or NO_2.[87,88] Phosphorous (P: $3s^2 3p^3$)-doped graphene (PG) in comparison to nitrogen would also obtrude out of the plane when doped in graphene, conserving its sp^3 character and bond with three neighboring C atoms in a pyramidal-like structure.[89,90] Substitutional doping with P can increase the chemical reactivity of PG. It would effectively reduce NO_2 into NO and could chemisorb with moderate adsorption energy. Chalcogenides, sulphur-doped graphene (Sul-G) (S: $3s^2 3p_x^2 p_y^1 p_z^1$) exhibits larger chemisorption energy compared to sulphur-doped carbon nanotubes. A Sul-G semiconductor material has a smaller band gap, due to structural changes. It show significant potential for gas sensing and selectively binding to NO_2 to trigger a change in the conductivity properties of the system.[91] Oxygen-doped graphene (Ox-G) (O: $1s^2 2s^2 2p_x^2 p_y^1 p_z^1$) showed more electronegativity and larger size compared to carbon-doped graphene, revealing that substitutional doping with O atoms is impossible. However, with epoxy (C–O–C) and carbonyl (C=O–C) groups, GO and rGO are in general regarded as O-dopant graphene. The covalent attachment of oxygen groups to graphene transforms sp^2 into the sp^3 hybridization state, accompanied by local distortion of the graphene planar structure. The extensive presence of localized sp^3 domains gives rise to the opening of the band gap.[92,93] This phenomenon together with the defects results in poor conductivity but results in excellent hydrophilicity. Halogen-doping transforms sp^2 carbon bonding to sp^3 hybridization, resulting in drastic distortions in the geometric and electronic structures of graphene. Fluorine (F: $1s^2 2s^2 2p^5$) being one of the most reactive elements, undergoes strong and inert bonding. The F–C bond in F-doped graphene obtrudes from the basal plane and stretches the C–C bond length to 1.57–1.58 Å.[78] Fluorine having a high affinity for C enables negative chemisorption energy in fluorine-doped graphene (F-G) semiconductors[94–96] with tunable band gaps, resulting in luminescence ranging broadly from ultraviolet to visible-light regions.[97] F-doping also increases the hydrophobicity of graphene.[98] A chlorine-doped graphene (Cl-G) (Cl: $3s^2 3p^5$) complex has a lower binding energy and longer bond length than fluorine or hydrogen, so the covalent Cl–C bond is less stable than C–F or C–H.[99] Due to its long bond length, Cl-G (1.1–1.7 nm) is thicker than F-G.[100] In contrast to a similar bonding arrangement like F, Cl can interact with C through the formation of a charge-transfer complex, covalent bonding and physical absorption.[101] Unlike F and Cl, Br and I are larger sized atoms, likely to interact with graphene only through physisorption or the formation of a charge transfer complex, without disrupting the sp^2 carbon network.[102] Brominated graphene is reported to be an indirect gap material with an almost zero band gap.[94] The electronegative and chemically reactive properties of iodine (I) facilitate easy aggregation to form linear poly-iodide anionic species (I^- and I^-) on the graphene surface.[103,104]

Co-doping of multiple species of foreign atoms into graphene can generate new properties or create synergistic effects. The similar sizes of B and N atoms produce opposite doping effects on graphene. When B and N are doped into graphene simultaneously, phase separation between boron nitride and carbon takes place,[105–109] attributed to the larger binding energies of (B···N) and (C···C) than those of (B···C) and (N···C)

bonds, respectively. Boron–nitrogen co-doping leads to four binding configurations: (C···C), (B···N) (dominant form), (C···B) and (C···N), with bond lengths of 1.42 Å, 1.45 Å, 1.49 Å and 1.35 Å, respectively. This enhances strong charge polarization between B and N, producing active surface chemistry.[110] The thermal stability of B···N co-doped graphene has been found to be lower than that of N-doped graphene, but higher than that of B-doped graphene.[111] Co-doping of graphene with a controlled B and N compositional ratio strengthens parameters like charge polarization, spin density and the conductivity of fuel cells, supercapacitors and batteries.[112] N/B, N/S and transition metal (Ni^{2+}/Ni^{3+}, Co^{2+}/Co^{3+} and Fe^{2+}/Fe^{3+}) co-doped reduced graphene oxide (CD-rGO) nanocomposites were successfully synthesized by a simple one-step hydrothermal approach and showed significant promotion of the catalytic oxidation of glucose for application in a direct glucose alkaline fuel cell (DGAFC). It was speculated that the boosted performance was due to the synergistic effects of N, S-doped rGO and metallic redox couples responsible for creating active sites and accelerating the electron transfer, respectively.[113] They reported the doping of N/S heteroatoms in rGO in addition to the Ni^{2+}/Ni^{3+} redox couple, which can play an important role in changing the electronic properties and chemical reactivity of reduced graphene oxide. C=C–N (graphite nitrogen) in a nickel-decorated N/S co-doped reduced graphene oxide nanocomposite (rGO-NS-Ni) can create more edges and defects on rGO-N/S covalently bonded rGO with pyrrol nitrogen and thiophene sulfur. These structures provided a larger electrolyte/electrode interface, resulting in smaller interface resistance, resulting in a high conductivity performance in rGO-NS-Ni, which can create more active sites in rGO by doping with N/S-decorated Ni transition metal compared to other redox couples Co^{2+}/Co^{3+} and Fe^{2+}/Fe^{3+}, respectively. The major problem in the glucose oxidation process at the DGAFC anode was the suppressed electron transfer process. Doping with a designed nanocomposite (rGO-NS-Ni^{2+}) was found to accelerate the electron transfer process, thus creating more active sites for electrochemical analysis. The addressed nanocomposite is considered to be an excellent system with better catalytic ability having maximum power density of 48.0 W m^{-2}, that was found 2.08 times higher than that of B having AC = 23.12 W m^{-2} respectively. In the case of asymmetric B/N doping, this could moderately increase the band gap (0.49 eV) because of symmetry breaking. This showed that at an appropriate B/N ratio, a reduced HUMO–LUMO energy gap can be created in graphene that can enhance the chemical reactivity[114] of the designed nanocomposite (G@B/N), thus creating a band gap at the Dirac point. Shifts in the Fermi level in the opposite direction are generated, providing uniform co-doping. In contrast, a scattered distribution of foreign atoms was also observed in the case of S/N co-doping that was predicted to show better catalytic activity compared to N/B co-doping.[115,116] Since the literature showing catalytic activity in the DGAFC anode *via* the designed transition-metal-decorated N/B co-doped reduced graphene oxide (rGO-N/B-M) nanocomposite is currently scanty; catalytic activities for such nanocomposites were reported for the oxygen reduction reaction (ORR) and oxygen evolution reaction (OER). This has widespread implementation in the field of new energy storage technologies. The insertion of N/B moieties can create active sites for transition metals that can exhibit high ORR in the whole system. Y. Irmawati *et al.*[117] reported a typically designed nanocomposite of iron-decorated N/B co-doped reduced graphene oxide (rGO-NB/Fe) as an electrocatalyst for ORR and OER systems, acting as alkaline and neutral electrolytes, respectively and creating active sites that can modify the electronic structure of rGO in the system. Thus, its applicability (3D porous structure) as graphene aerogels with N/B moieties, with Fe-decorated nanocomposite, for a highly stable Zn–Air battery (34 mW cm^{-2} in power density and remaining stable for 284 h; ~852 cycles) was acclaimed.

3 Synthetic methodology for the functionalization of graphene and its derivatives

The synthetic approach for the effective preparation of graphene and its derivatives depends on the requisite size, purity and efflorescence of individual graphene materials required for target applications. Various recommended synthetic approaches that have revealed modified stable structural formation of graphene and its derivatives are reported in Fig. 4. Most of these routes are either top-down or bottom-up

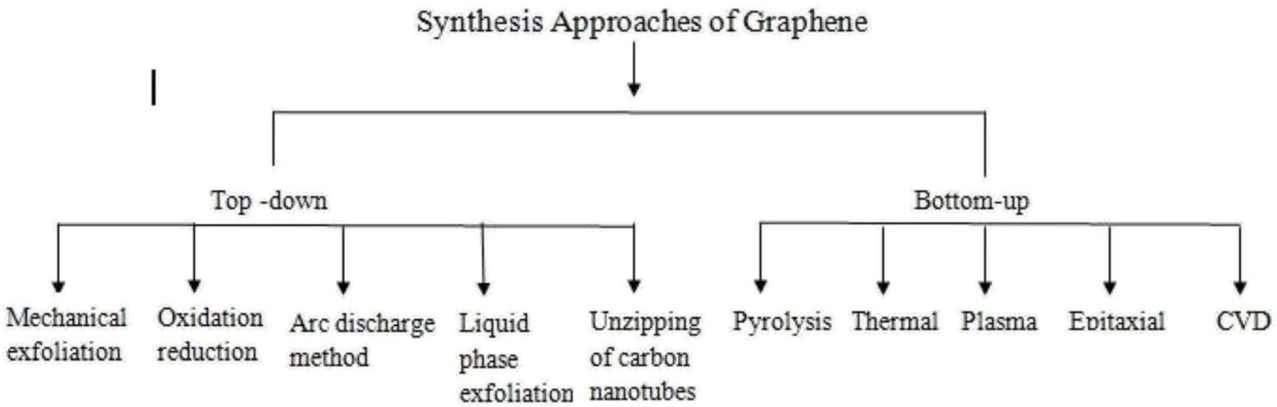

Fig. 4 Synthesis approaches adopted for the preparation of graphene and its derivatives.

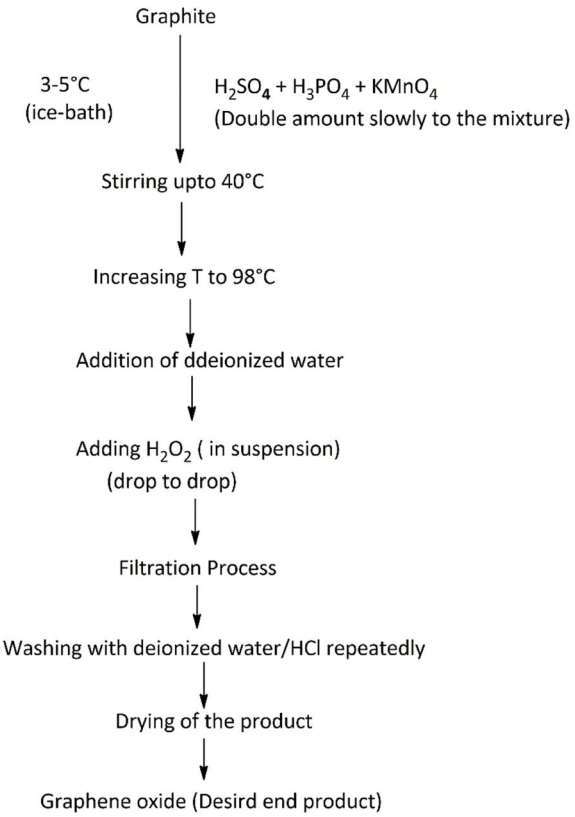

Fig. 5 Modified chemical reaction involved in the synthesis of colloidal graphene oxide.

approaches. The top-down approaches involve delaminating of graphitic materials, whereas the bottom-up approaches involve graphene assembly from smaller building units. In general, the top-down approach involves exfoliation and reduction methods. These methods require precursors in gaseous form to allow deposition onto the metal surface. Mechanical exfoliation includes techniques such as micro-mechanical cleavage, continuous mechanical cleavage, shear exfoliation, and explosive exfoliation, which are often proffered. Chemical exfoliation includes liquid phase exfoliation (LPE) and supercritical fluid exfoliation. Conversely, electrochemical exfoliation, thermal exfoliation reduction and chemical/electrochemical reduction techniques are also in use. Colloidal graphene oxide (GO) is prepared by a modified Hummer's method, which is a significant top-down method. It is used for the large-scale synthesis of graphene-based composites. Its principal steps are: (i) oxidation of graphite in concentrated H_2SO_4 with H_3PO_4 and $KMnO_4$, (ii) the exclusion of excess $KMnO_4$ by reducing it to water-soluble $MnSO_4$ with H_2O_2 and (iii) lastly, washing with methanol. Various modifications and improvements have recently been extensively discussed by dedicated scientists in this niche area.[118] The modified chemical reaction involved in the synthesis of colloidal graphene oxide is illustrated in Fig. 5. A colloidal solution of nanoparticles of GO was synthesized first and was then reduced to graphene-nanocomposites (GNCs). The dispersion of GNCs with different surfactants/polymers and reducing agents, mainly hydrazine, sodium borohydride, ascorbic acid, ethylene glycol, ammonia, or alkali solution, has recently been investigated. The reaction has been subjected to various optimizations with respect to temperature and reaction kinetics. Metal ions or pre-functionalized metal nanoparticles react with GO surfaces through electrostatic interactions, covalent interactions or by weak interaction to form target nanocomposites. A schematic illustration of synthetic strategies for graphene (G)- and graphene oxide (GO)-based nanocomposites with different nanoparticles is reported in Fig. 6. Some recent studies on the chemical synthesis of graphene

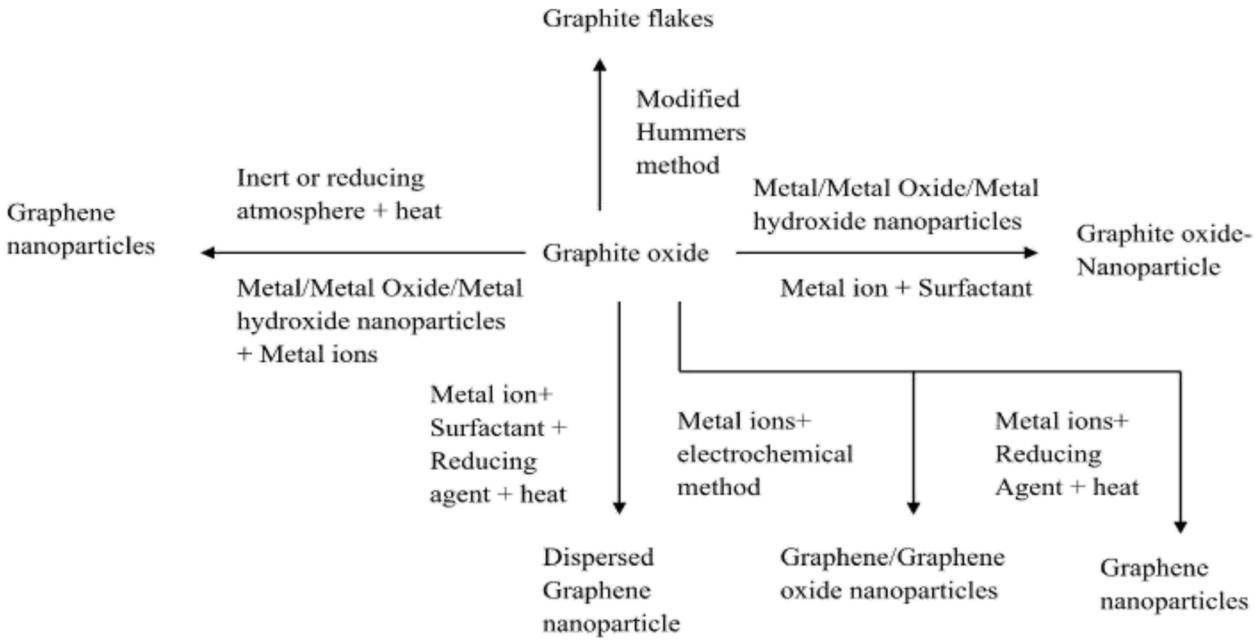

Fig. 6 Schematic illustration of synthetic strategies for graphene and GO-based composites with different nanoparticles.

Table 1 Recent studies on the chemical synthesis of graphene oxide reported in the literature

Materials used	Duration	Temperature	Specifications	Reference
K_2FeO_4, H_2SO_4, and graphite flakes	1 h	Room temperature	Used strng green oxidant, K_2FeO_4, avoided the use of polluting heavy metal like manganese and toxic gases in the preparation, enables the recycling of H_2SO_4 and elimination of the pollutants.	119
$KMnO_4$, $NaNO_3$, and H_2SO_4	16 h	10 °C	Formation of high quality r(GO) was formed reorganizing the carbon framework efficiently by controlling the reaction temperature upto 10 °C during successive oxidation steps; thereby preventing over-oxidation of graphene layers. reduction of graphene oxide to graphene at higher temperature than 1500 °C would cause the complete degradation of GO.	120
$KMnO_4$, $NaNO_3$, and H_2SO_4	<2 h	35 °C	Reaction time was found short, purification procedure reported in the work eliminated oxidative impurities, thereby, decreasing the thickness of nanoplatelets, similar oxidation degree of graphite oxide was observed as reported by chemical reduction technique.	121
H_2SO_4, $KMnO_4$, and H_3PO_4	12 h	50 °C	Exclusion of $NaNO_3$, resulted in the reduction of toxicity, improved efficiency of oxidation process was observed by increasing the concentration of $KMnO_4$ and 9 : 1 mixture of H_2SO_4/H_3PO_4, current modified method provided a greater amount of hydrophilic oxidized graphene material as compared to Hummer's method or Hummer's method with additional $KMnO_4$.	122
HNO_3	2 h	Room temperature	Oxidation of graphite to graphitic oxide was accomplished by treating graphite with essentially a water-free mixture of concentrated sulfuric acid, sodium nitrate and potassium permanganate, entire process required less than two hours for completion at temperatures below 45 °C. Temperature limitations and safely was successfully maintained.	123

oxide are reported in Table 1.[119–123] Other derivatives of graphene like fluorographene have been synthesized by reacting graphene with either XeF_2 (ref. 31, 97 and 124) or CF_4 (ref. 125) at room temperature by mechanical or chemical exfoliation of graphite fluoride.[94,96] A sonochemical exfoliation process of graphite fluoride in *N*-methyl-2-pyrrolidone (NMP) at ambient temperature[126] has been carried out in addition to the reaction of graphene oxide with HF, under hydrothermal conditions using an ultrasonication process.[127] The synthesis of graphyne is done using modern acetylene chemistry, which has been advanced by powerful new organometallic synthetic methodologies, proposed by Diederich in 1994. Being receptive to unusual methods produced by other disciplines is also to be encouraged.[128] In 2008, Haley presented the synthetic strategies and optoelectronic properties of the substructures of the non-natural, planar carbon networks of graphyne, which is based on the dehydrobenzoannulene framework.[27,129] He pointed out the necessity of extensively developing and utilizing metal-catalyzed cross-coupling, homo-coupling, and metathesis reactions to synthesize targeted products. The future synthesis of graphyne materials may involve the use of surfaces as supports and templates. Graphdiyne represents a promising material due to its attractive electronic, optical and electrochemical properties deriving from its unique molecular structure. Graphdiyne is synthesized as a nanotube array using an anodic aluminum oxide film template with a channel diameter of 200 nm and a Cu catalyst. Graphdiyne nanotubes with length 40 mm and wall thickness of 40 nm have been reported.[130] In bottom-up techniques, chemical vapour deposition (CVD), epitaxial growth and pyrolysis are quite common.[131,132] For the CVD method, a vacuum is specifically required, ensuring that reactants reach the substrate without any interference. The substrates for each method differ with CVD, requiring specifically a transition metal substrate. Chemical vapor deposition is a non-wet-chemical method used for the production of graphene. Pyrolysis and epitaxial growth do not require vacuum conditions, thereby indicating lower fabrication cost. Spray pyrolysis utilizes a glass substrate, and the epitaxial growth, on the other side, uses silicon carbide. Generally, quality graphene is synthesized by a micro-mechanical exfoliation technique on a silicon substrate or by a chemical vapour deposition method on transition metal surfaces; however, these methods have low production efficiency. The literature reveals that graphene flakes can also be obtained by mechanical cleavage using adhesive tape.[53] These flakes have to be placed on an Si wafer with a 300 nm thick layer of SiO_2, which are visible with a high-resolution optical microscope.[133] Graphene from SiC (epitaxial growth) can also be produced. However, the isolation of graphene remains a complex procedure.[134,135] In 2009, cold hydrogen plasma using argon was mixed with 10% hydrogenation at a low pressure of 10 Pa and a temperature of 4–160 K.[42] The hydrogenation transformed highly conductive semimetallic graphene (zero overlap) into insulating graphene. The reaction was observed to be reversible by plasma irradiation and annealing. Hydrogenated graphene is also formed by electrolytic hydrogenation of thin graphene flakes in the presence of water at room temperature, by applying 10 V and a current of 2×10^{-3} A.[136] It was observed that even exfoliation of graphite

Table 2 Various approaches for the production and extraction of graphene that depend on the requisite size, purity and efflorescence

Methodology	Specification/advantages/disadvantages	References
Bottom up methods		
Epitaxial treatment	Possibility of epitaxial growth of graphene on silica carbide, thermally used for silicon fabrication technologies, electrochemical detection of heavy metal salts in sea water, reduced cost, allowing seamless integration/bulk production of SiC substrates, reflects limitations in terms of costs, sizes, and difficulty in conduct.	139 and 140
Thermal treatment	Production of thermally reduced graphene from graphene oxide, remarkable source for polymer electrolyte membrane for fuel cells applications, reduction causes significant weight loss and volume expansion of the materials. Reduction of GO is mainly concerned with the elimination of hydroxyl and epoxy groups; other groups like carbonyl, carboxylic and ester groups exhibit no significant role in conductivity.	141 and 142
Plasma treatment	Used in cleaning the surface material, etching, deposition and modification of the surface properties of the material, potential hinge in hydrophilicity, adhesion, conductivity, functionalization, reduction, and doping of GO, necessary for the correct selection of promising parameters in order to reduce the negative impacts.	143 and 144
Pyrolysis treatment	Used for the formation of thermally induced chemical decomposition of organic materials in the absence of oxygen, resulting in the production of carbon materials, however, presence of oxygen within the paralyzing precursor leads to partial combustion of the material.	145
Chemical vapor deposition	Involves the process of depositing material as a thin film onto the substrates from vapour species through chemical reactions, the method is suitable for the growth of graphene for the solid, liquid and gaseous carbon sources, helps monitoring various factors affecting the quality of graphene film, however, the growth process is a tedious process due to the required maintanance of system total pressure, partial pressure of hydrogen, presence of hydrocarbon species, growth temperature and source of power respectively.	146
Topdown method		
Liquid-phase exfoliation	Method helped in obtaining a stable dispersion of monolayer or few-layer defect-free graphene, direct exfoliation prevented the agglomeration of the nano sheets, however, the method only involves the exfoliation of natural graphite *via* high-shear mixing or sonication, suffers from high energy extensive consumption and low efficiency.	147 and 148
Modified unzipping of carbon nanosheets	Method is used in the production of graphene nano-ribbons, reflects the reduction of the oxygen-functional groups at the ends of graphene basal planes, reduction in electrical conductivity, adjustment achieved in the reduction step is observed, reduced consumption of chemicals make the overall process more economic and eco-friendly, however, harmful effect of the oxygen-functional groups take place at the edges of the graphene sheets and on the properties of the prepared material.	149
Arc discharge method	Anode and cathode are submerged in a gas or liquid medium of a reaction chamber, use of asphalt a carbon rich source is used, makes the method cost effective due to vacuum usage.	150
Oxidation reduction	Method is usally used in the synthesis of graphene from graphite, oxidation of graphene increases the interlayer spacing of graphite layer due to incorporation of intercalation compounds, graphene is found devoid of any functional groups and thus is found insoluble in water and organic solvents.	150

oxide (6 to 15 MPa) at high hydrogen pressure and between 200 and 500 °C resulted in partially hydrogenated graphenes.[137] Even at high temperature and pressure (400 to 500 °C, 5 MPa), hydrogenation resulted in the partial hydrogenation of single-volt carbon nanotubes, where unzipped graphene nanoribbon formation has been observed.[138] However, recent approaches for the production of graphene depending on the requisite size, purity and efflorescence are reported in Table 2.[139–150]

4 Functionalization of graphene leading to its enhanced structural versatility

Extensive valuable research is presently under progress, in the fields of synthesis, property identification and characterization for graphene and graphene oxide. Due to the addition of oxygen atoms bound with a few carbons (Fig. 7), G/GO reflects different physico-chemical and thermo-physical properties. Graphene oxide being hydrophilic is easily dispersed in water. It contains aromatic (sp^2) and aliphatic (sp^3) domains, which leads to an increase in specific interactions occurring on its surface. Graphene oxide can be reduced to graphene in a reverse manner by a moderate reducing agent. However, the produced graphene is not suitable for electronic applications and mechanical reinforcement with polymers due to structural defects created during the synthesis of graphene oxide. Thus, proper functionalization of graphene and graphene oxide is essential to prevent their aggregation and inherent physico-chemical properties during the reduction process. Methods for the functionalization of graphenes and graphene oxide include: (a) covalent functionalization, (b) non-covalent functionalization and (c) elemental doping.

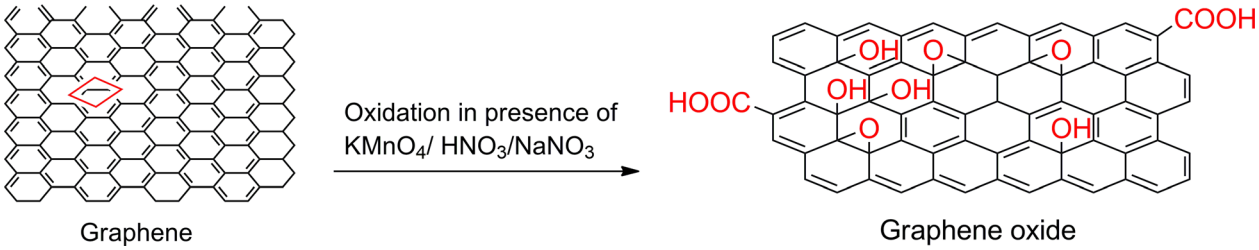

Fig. 7 Oxidation reaction of graphene sheet to synthesize graphene oxide.

4.1 Covalent bond functionalization

Covalent bond functionalization of graphene with newly introduced groups in the form of covalent bonds can be used to improve and enhance its chemical performance. O-containing groups on the surface of GO make covalent bond functionalization easier than that on graphene. The surface of graphene oxide contains a large amount of epoxy groups (Fig. 8),[151] hydroxyl groups (Fig. 11),[152] and carboxyl groups (Fig. 12).[153] These groups can be used for chemical reaction such as

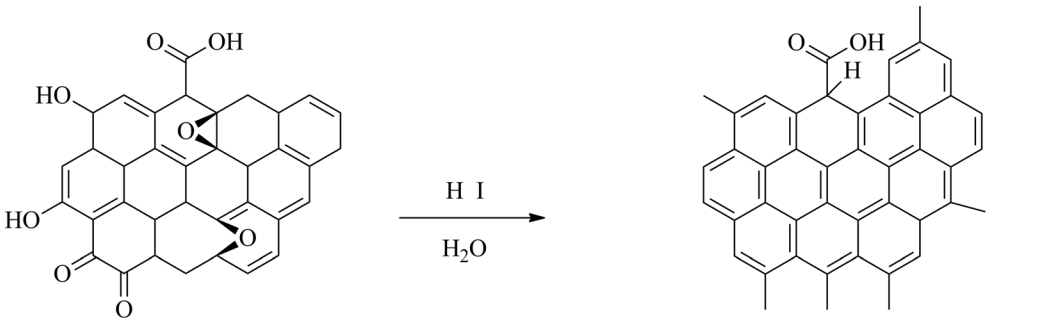

Scheme 1: Mechanism of epoxide reduction

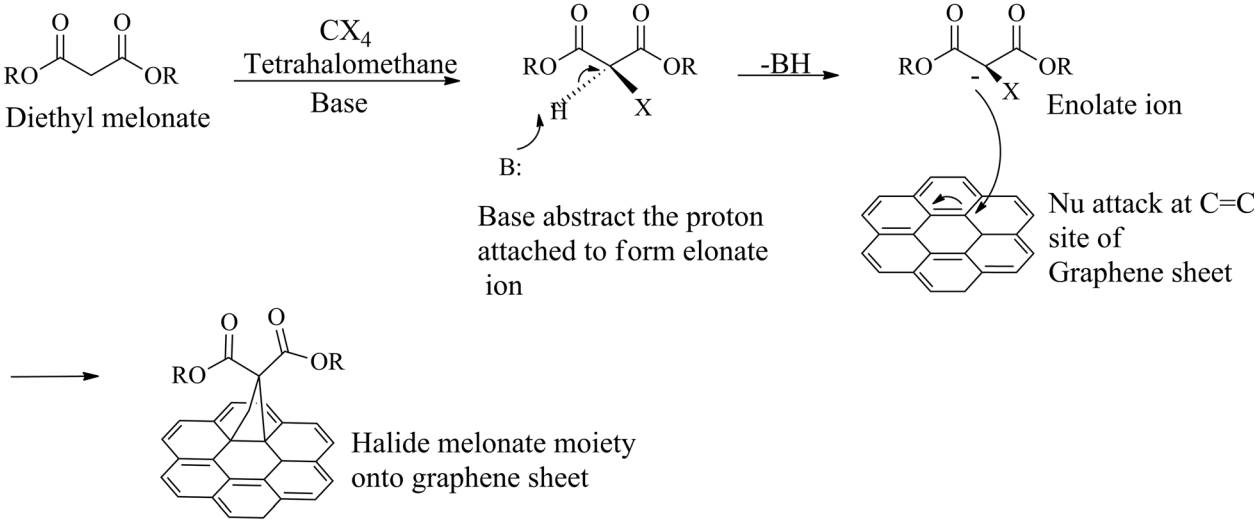

Scheme 2 : Mechanism of formation of halide melonate moiety onto graphene sheet

Fig. 8 Mechanism of the top formation of halide derivatives of enolate (bottom) addition of halide derivative of enolate onto graphene.

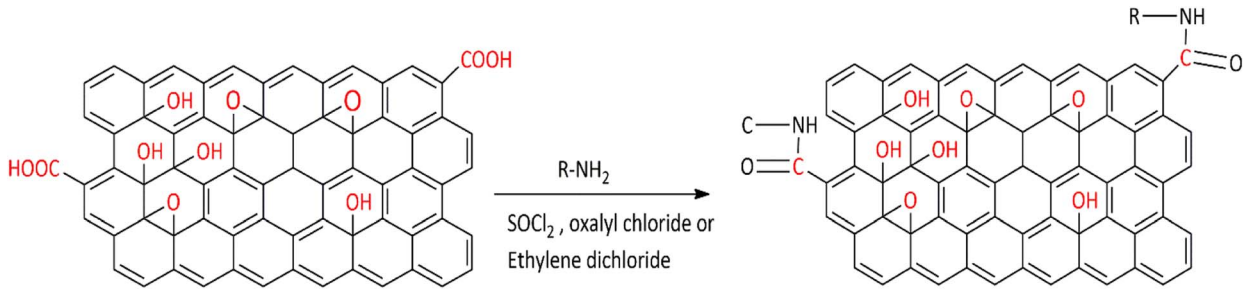

Fig. 9 Illustration of the isocyanation reaction of EDC-*N*-(3-dimethylaminopropyl)-*N*′-ethylcarbodiimide hydrochloride on graphene oxide sheets.

isocyanation (Fig. 9),[154] diazotization and addition (Fig. 10),[155] carboxylic acylation (Fig. 12),[153] and epoxy ring opening (Fig. 8).[151] Three types of covalent bond functionalization are:

4.1.1 Carbon skeleton functionalization. Graphene can also undergo functional modification of the carbon skeleton. This is carried out using carbon–carbon double bond (C=C) sites involved in the aromatic ring of graphene or graphene oxide. The concept can best be illustrated by the diazotization reaction and Diels–Alder reaction (Fig. 10).[155] Solution-phase graphene as a raw material is dispersed in an aqueous solution of surfactant, 2% sodium cholate followed by stirring with 4-proparglyoxydiazobenzenetetrafluoroborate at 45 °C to obtain functional graphene, 4-propargyloxyphenyl graphene (GC≡CH). This may be a perfect example of functionalization of graphene exhibited by a click chemistry reaction with the help of azido polyethylene glycol carboxylic acid, to illustrate the addition reaction to the skeleton carbon structure of graphene, reflecting advanced functionalization of a graphene sheet. The final product can be used to make efficient and robust biosensors.

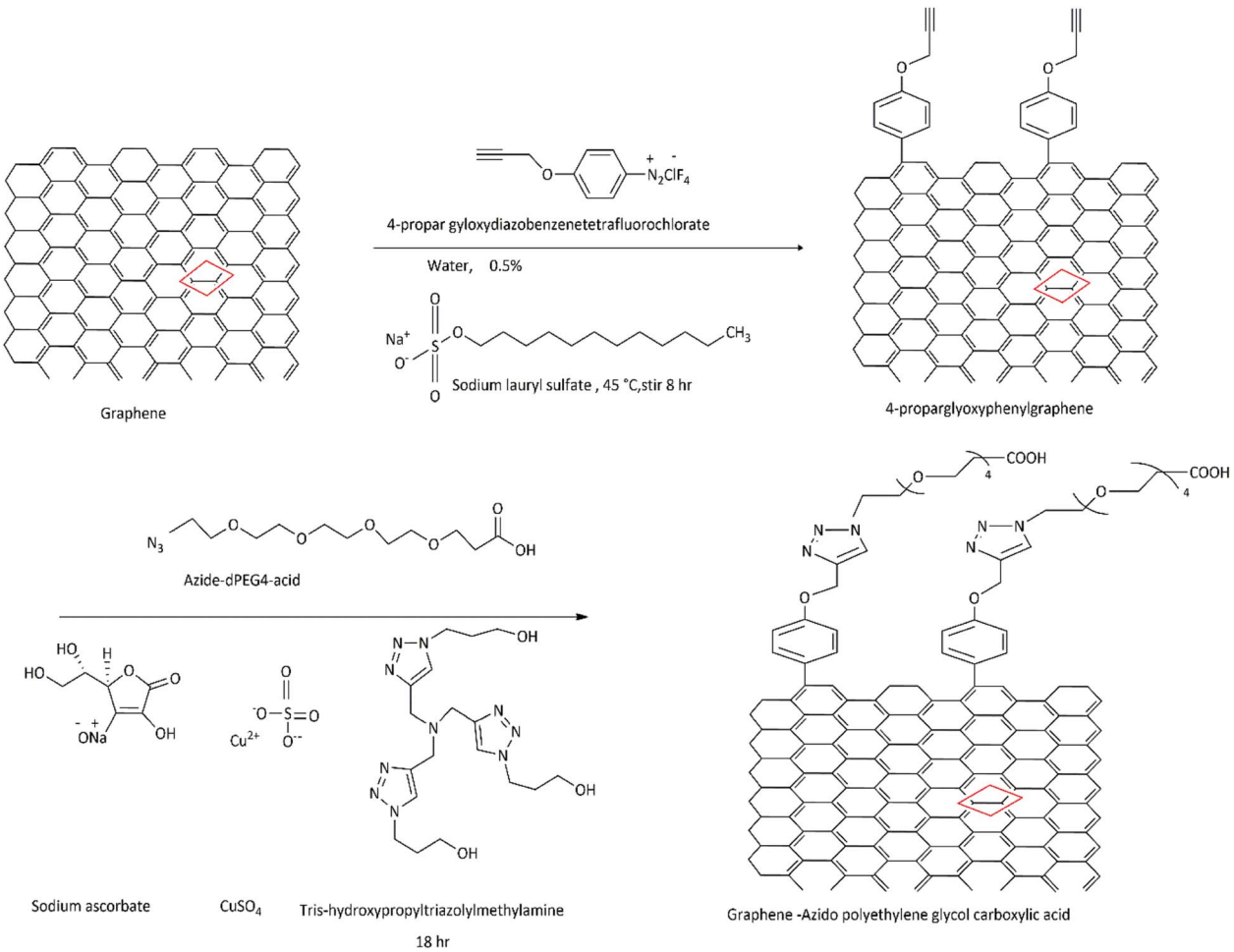

Fig. 10 Diazonium reaction and subsequent click chemistry functionalization of graphene sheets.

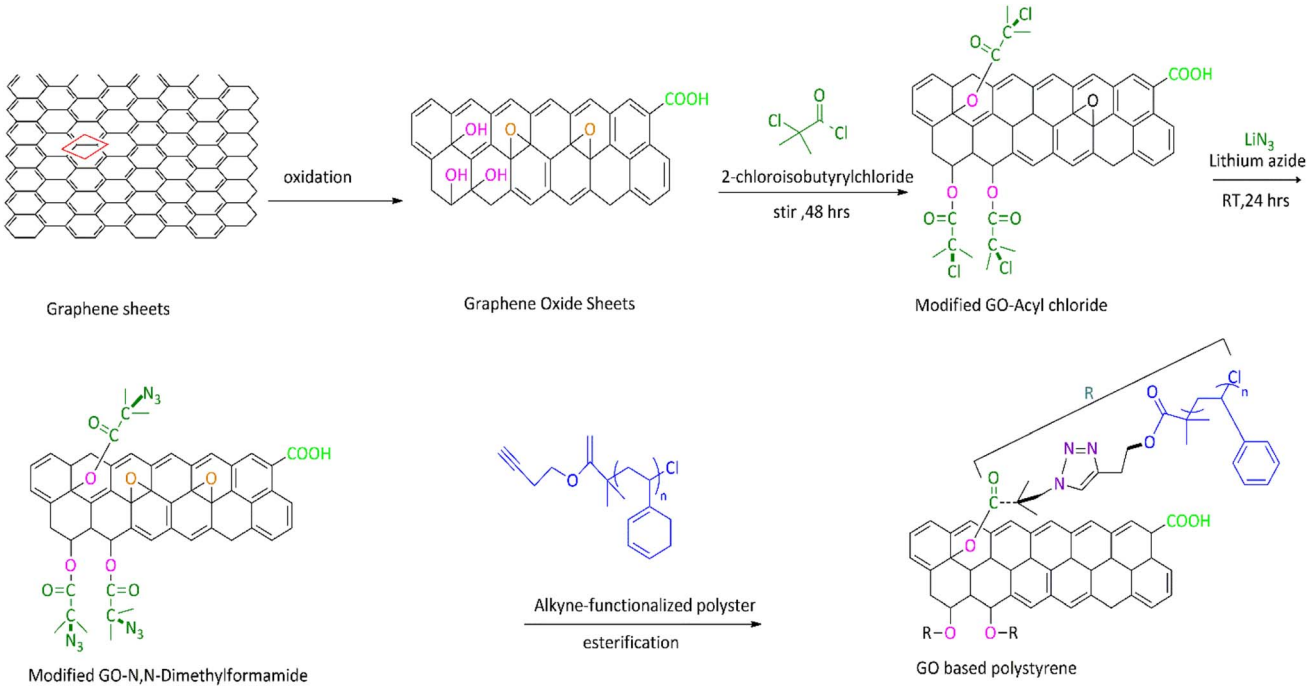

Fig. 11 Synthetic route of polystyrene graft graphite oxide (GO/PS).

4.1.2 Hydroxyl functionalization. Covalent linkage of hydroxyl groups over the surface of graphene oxide sheets results in the removal of H-groups from the surface. Subsequent chemical combination of polystyrene and graphene under weakly basic conditions and covalent linkage within polystyrene modified graphene oxide is illustrated in Fig. 11.[152] Here, an S_N2 nucleophilic substitution mechanism is taking place. This represents an interesting potential alternative method for the synthesis of novel composite materials with interfacial interaction, leading to the formation of smart carbon-based nanocomposites and their applications[152]

4.1.3 Carboxyl functionalization. The carboxyl functionalization step is regarded as the activation step of the reaction. The carboxyl groups on the edges of graphene oxide are in fact highly reactive groups. As a result, the moiety containing a hydroxyl group or an amino group is dehydrated to form amide and ester bonds. A few of the commonly used activation groups are 2-(7-aza-1*H*-benzotriazole-1-yl)-1,1,3,3-tetramethyluronium hexafluorophosphate[156] thionyl chloride, *N*,*N*-dicyclohexylcarbodiimide (DCC),[157] and 1-ethyl-3(3-dimethylaminopropyl)-carbodiimide (EDC).[158] Fig. 12 reveals a simple and quick GO functionalization group interconversion, followed by two sequential copper acetoacetate (CuAAC) clicks for double GO functionalization.[153]

4.2 Non-covalent functionalization

The non-covalent bond functionalization of graphene and graphene oxide results in the formation of a composite material with interaction between hydrogen bonds and electrostatic forces between graphene and functional molecules. This results in an improvement in dispersibility and stability of graphene and graphene oxide in the reaction medium. Under mild conditions, the non-covalent bond functionalization process is quite simple as it maintains the structure and properties of graphene. The process is carried out using specific surfactants. The functional modification of the surface of non-covalent bonds primarily involves: (i) π–π bond interaction, (ii) ionic bonding, (iii) electrostatic interaction, and (iv) hydrogen bonding modification.

4.2.1 π–π bond interaction. Depending on the available orientation of π-systems and geometry (planarity) of interacting species between targeted aromatic molecules, π–π interactions can be introduced during exfoliation of graphite alone. Electron-donating groups,[159–161] dopant concentration[161] and type of substituent of the graphene sheets[162] greatly influence the π–π interactions. Additionally, the number of sheet layers,[158] withdrawing ability, and size, besides the planarity of the aromatic molecules greatly influence the π–π interactions.[163–166] Chia *et al.*[167] reported the functionalization process of a graphene surface *via* the π–π bond interaction. Fig. 13 illustrates such interactions occurring over screen-printed electrodes on exfoliated graphene sheets. This involves the binding of a succinimidyl ester moiety with amine groups in the enzyme glucose oxidase. Fig. 13 illustrates the schematic representation of the functionalization of pristine graphene sheets with 1-pyrenebutyric acid *N*-hydroxysuccinimide ester on its surface. A well-established mediation between graphene and flavine adenine di-nucleotide sites of the glucose oxidase enzyme is observed. Zhang *et al.*[168] reported that a dispersion of graphene-based material, with characteristic aggregation-induced emission (ALE) (the photoemission property of fluorescent dyes) can be synthesized by wet-chemical

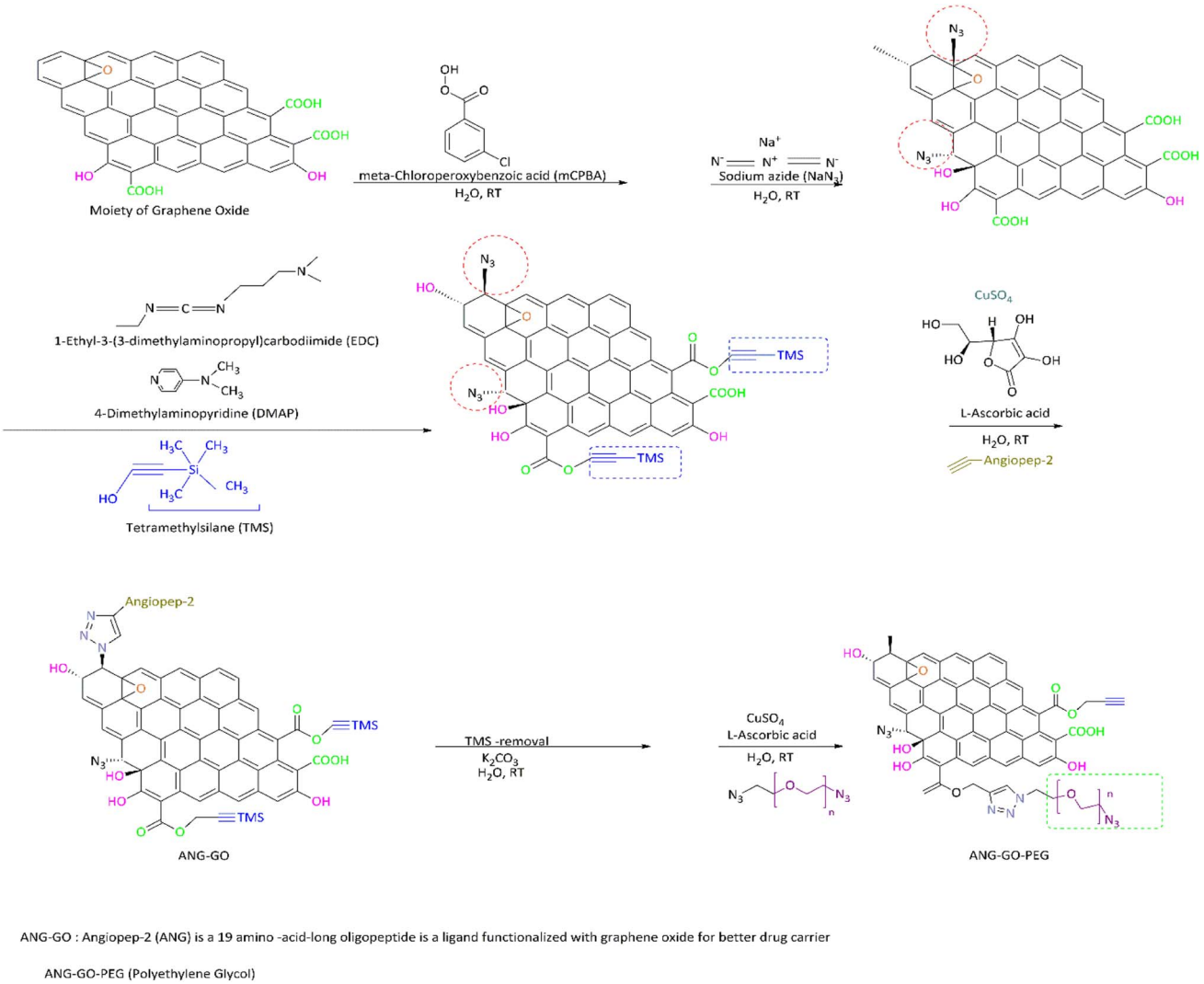

Fig. 12 Sequential functionalization of GO using two CuAAC click reactions.

reduction of GO. During the reduction interval, a conjugate molecule containing tetraphenylethylene and pyrene (TPE-P) was used as a stabilizer to establish the π–π interaction and thereby the wrapping effect. The resultant synthesized reduced graphene oxide-tetraphenylethylene and pyrene (rGO-TPE-P) products not only have good dispersibility in solution but also show photo-luminance characteristics. This enables rGO-TPE-P to be used as a chemical sensor for highly sensitive explosive detection. Zhang *et al.* applied the product as a chemical sensor for detecting trace 2,4-dinitrotoluene (DNT) at concentrations lower than 0.91 ppm with a quenching constant as high as 2.47 $\times 10^{-4}$ M^{-1} in the aggregated state (Fig. 14).[168]

4.2.2 Ionic and electrostatic interactions. These interactions play a significant role in the functionalization of graphene. They play a vital role in establishing a bond between a surfactant and pristine graphene nanosheets. Several researchers, particularly, Choi *et al.*[169] and Ge *et al.*,[170] revealed an improvement in the stable dispersion of reduced graphene *via* various organic solvents, as a result of non-covalent ionic interaction functionalization with amine terminals and polymers of sodium dodecyl benzene sulfonate (SDBS). The protonated amine of the terminal groups of polystyrene undergoes non-covalent functionalization with the carboxylate group on the graphene surface, resulting in high dispersibility in various organic media. The mechanism is illustrated in Fig. 15. Conversely, the hydrophilicity of SDBS-functionalized reduced graphene resulted in good dispersion in an oxidized starch matrix. It revealed better mechanical and barrier properties for the fabricated starch film. The tensile strength of reduced graphene oxide/oxidized starch (r-RGO-4/OS) film was found to increase to 58.5 MPa, which was three times higher than that of the oxidized starch film (17.2 MPa). The modified films of rGO/OS have wide applications in optoelectronics. These films can effectively protect against UV light due to their light-proof performance. These composite modified films also have great potential in packing industries. Besides ionic interactions, electrostatic interactions also play a vital role in the dispersion of graphene. Graphene oxide and reduced graphene oxide, when dispersed in aqueous solution, also behave like a 2D conjugated polyethylene. This is because the surfaces

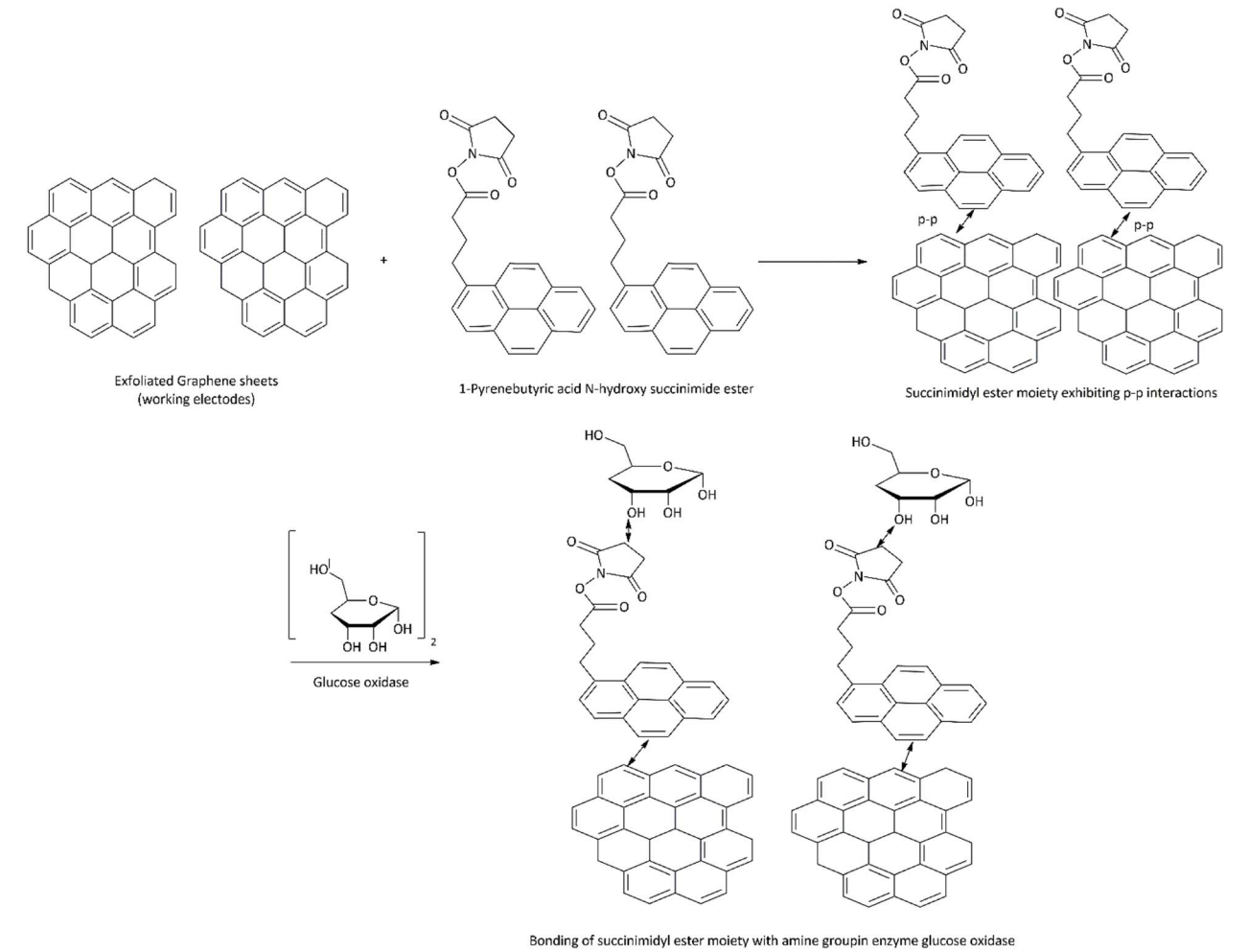

Fig. 13 Schematic representation of exfoliated graphene sheets with 1-pyrenebutyric acid *N*-hydroxyl succinimide ester mediating between graphene and redox sites of glucose oxidase enzymes.

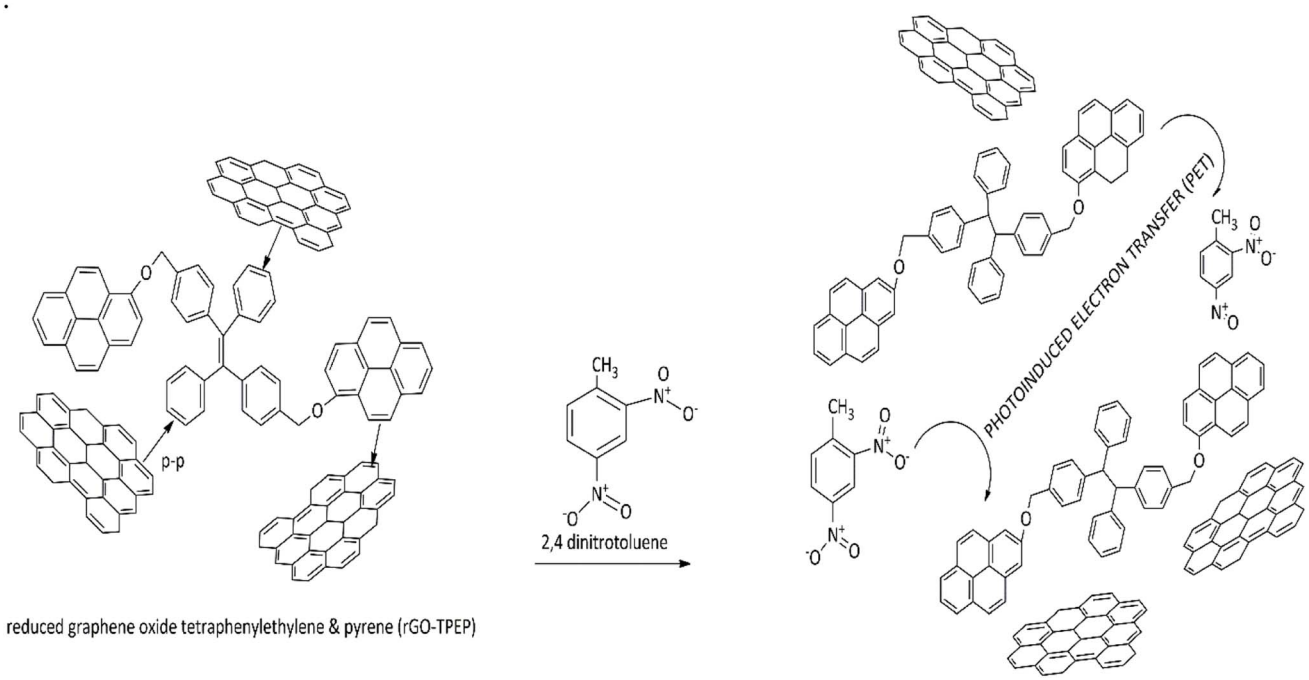

Fig. 14 Mechanism of detection of explosive DNT *via* rGO–TPEP.

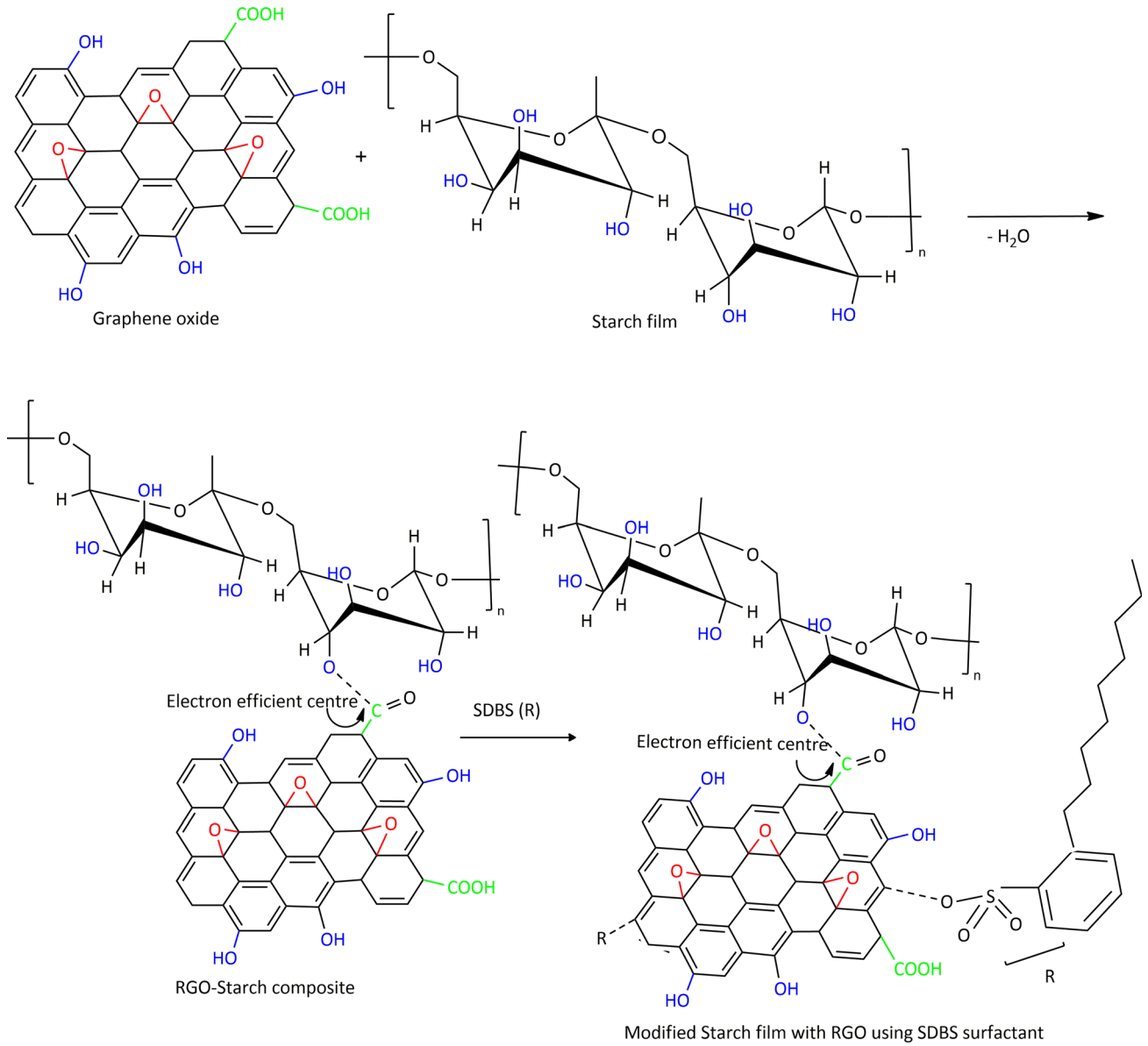

Fig. 15 Illustration of the mechanism of modified starch film with reduced graphene oxide by SDBS surfactant.

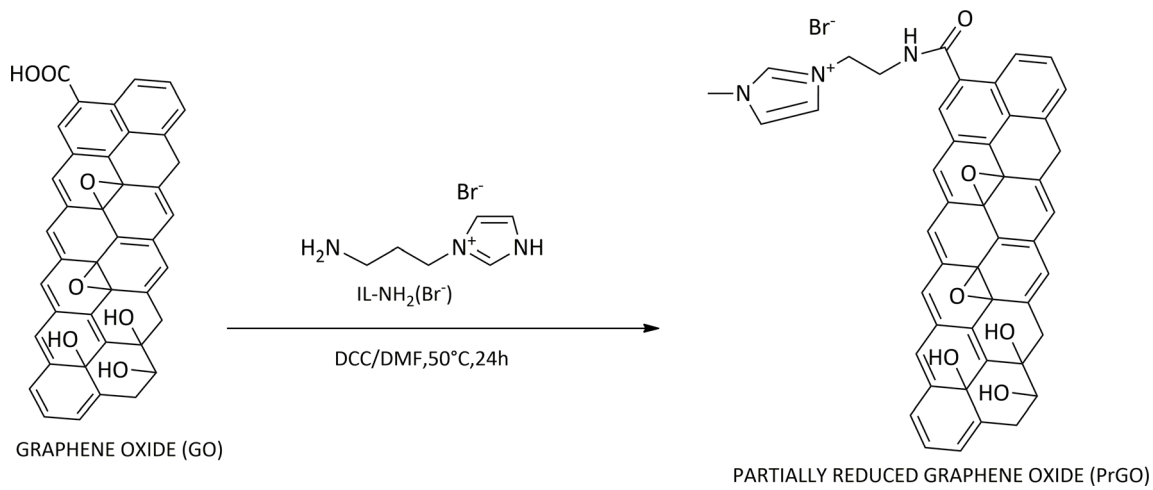

Fig. 16 Illustration of the mechanism involved in chemically modified graphene oxide as partially reduced covalently bonded graphene oxide (PrGO).

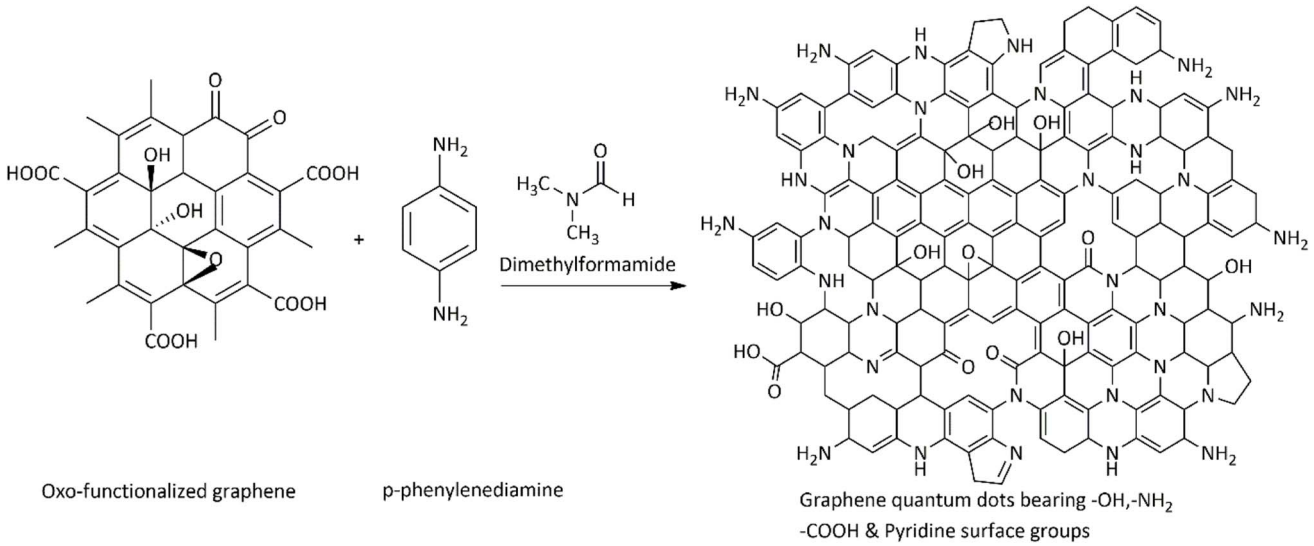

Fig. 17 Schematic diagram for the synthesis of GQDs with surface functionalities.

carrying negative charges on which cationic aromatic derivatives can assemble through electrostatic repulsion (which can only take place between same charges), helping to improve the dispersion of graphene.[171,172] The literature reveals that Bhunia *et al.*[173] reported chemically modified graphene oxide as partially reduced graphene oxide (PrGO), which is covalently bonded with an ionic liquid (i^L) for homogeneous dispersion, in polar aprotic organic solvents like *N*-methyl-2-pyrrolidone (NMP) and *N*,*N*-dimethylformamide (DMF). 1-(3-Aminopropyl)-3-methyl imidazolium bromide was used as a reducing agent

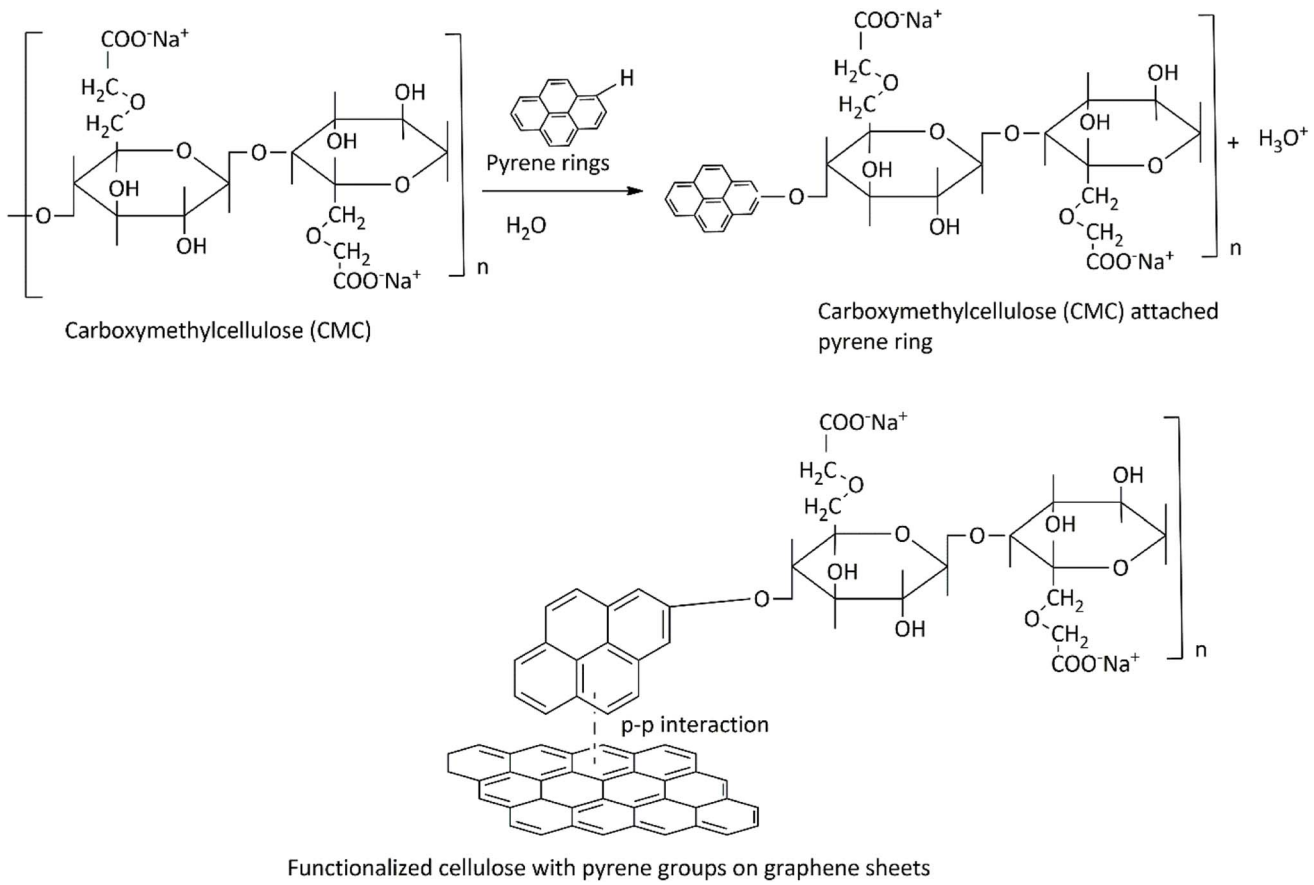

Fig. 18 Mechanism of functionalization of graphene sheet with pyrene derivative of cellulose.

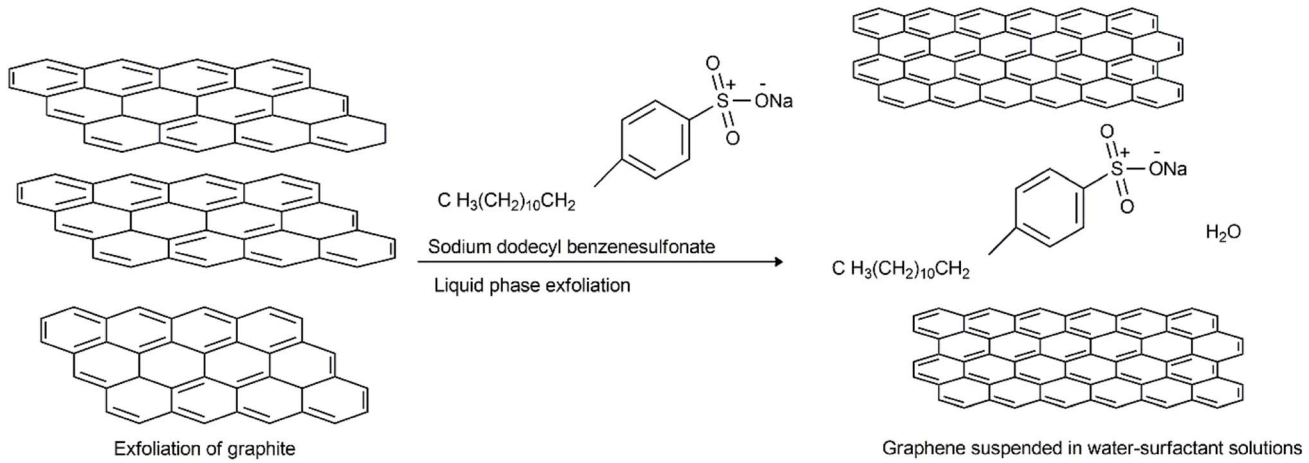

Fig. 19 Modified method to disperse graphite in surfactant-water solutions (SDBS in water) through sonication.

to control the reduction while removing functional groups such as hydroxyl groups and epoxy bonds of graphene oxide. The carboxylic functional groups of PrGO at the edges through amide coupling were retained. In general, GO is an insulator, but chemically modified and partially reduced GO, more accurately PrGO–(i^L), is capable of showing a charging effect, leading

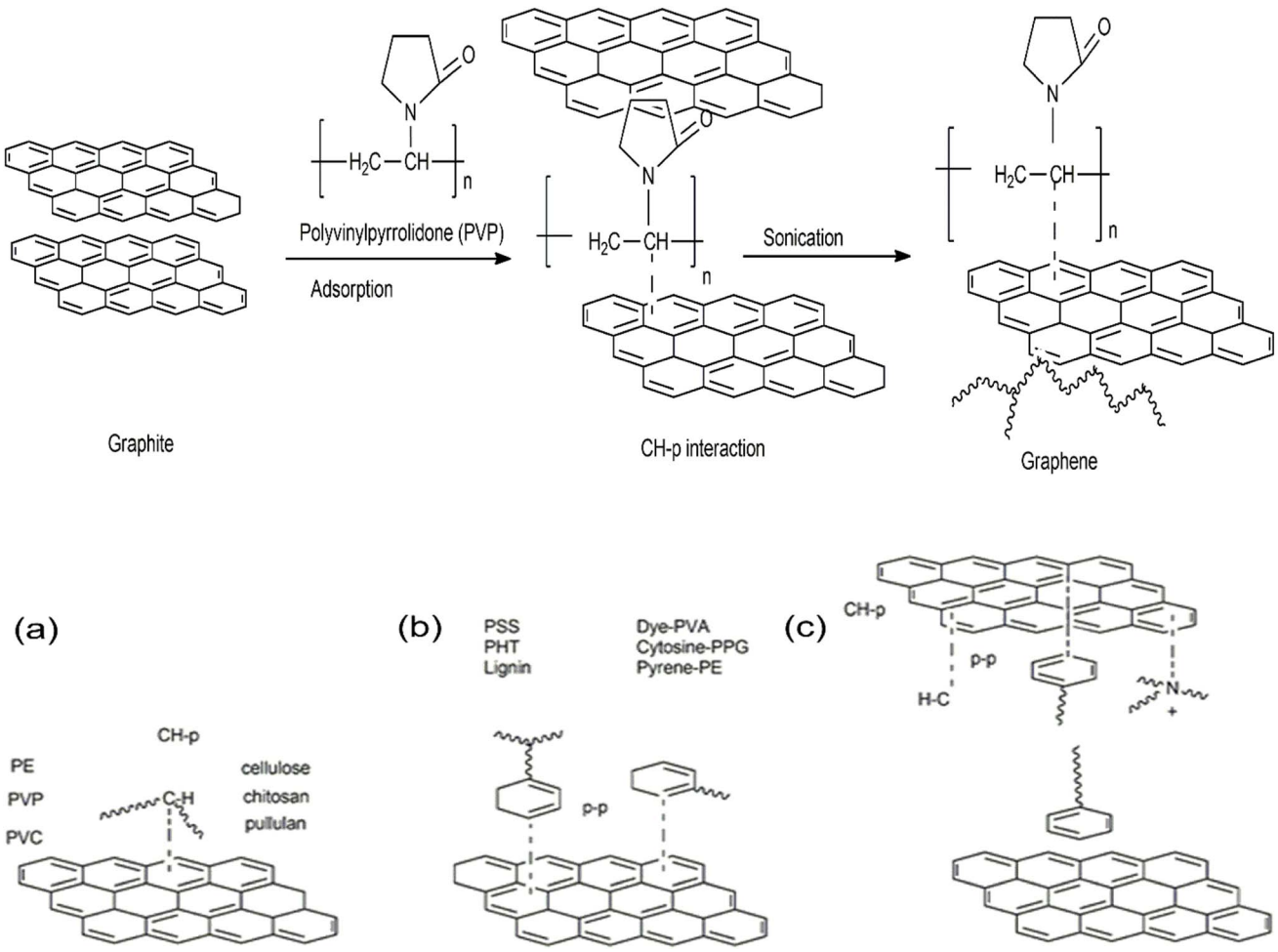

Fig. 20 Crystalline graphite powder with an aqueous solution of PVP under sonication which resulted in water-soluble polymer-protected graphene single layer. (a) CH–π bonding under polyethylene (PE), polyvinylpyrrolidone (PVP) polyvinylchloride (PVC), cellulose, chitosan and pullulan treatment, (b) π–π stacking (under poly(3,4-ethylenedioxythiophene (PSS), polyhexahydrotriazine (PHT), lignin, dye-polyvinyl alcohol (dye-PVA), cytosine-polypropylene glycol (cytosine-PPG) and pyrene-polyethylene (pyrene-PE) treatment and (c) cation–π interaction.

to switching and memory properties according to the movements of counter anions. The mechanism of this reaction is illustrated in Fig. 16.

4.2.3 Hydrogen bonding modification. Apart from the aromaticity of G involved in the π–π interaction, as discussed above, it is also characterized by its hydrophobic or partially hydrophobic behavior. As a result, G can undergo reaction with hydrophobic or partially hydrophobic organic molecules, such as the surfactants, ionic liquids and macromolecules. These interactions are mostly used to promote the dispersion of G-sheets in aqueous as well as organic media or even in identified polymers. The hydrophobic interaction of G/rGO with aliphatic sites of the surfactants enhances their stability in water. The hydrophilic parts of the surfactant responsible for the interaction are mostly anionic macro-molecules, highly polar groups or zwitterions.[174] Hu *et al.*[175] reported the favorable influence of solvent proticity on the optical properties of graphene quantum dots, ascribed to the presence of $-NH_2$, –OH, and –COOH on the graphene quantum dot (GQD) surface, which undergo hydrogen bonding interaction that may lead to the rigidity or fixation of these surface groups (Fig. 17). Apart from above detailed functionalization methodologies, it has been identified that cellulose derivatives, lignin, albumin,[176–178] sodium dodecyl benzenesulfonate (SDBS),[179] sodium cholate[180] and polyvinylpyrrolidone (PVP) are some of the few amphiphilic organic molecules/macromolecules, which can act as potential graphene dispersants and stabilizers. Sodium carboxymethyl cellulose, a natural polysaccharide, when bonded to graphene, helps it to achieve stability and thus enhances its stable water dispersion. No doubt, in this case π–π stacking is not involved, since cellulose is totally aliphatic. It is hydroxyl propyl cellulose that is able to disperse reduced GO, resulting in a unstable

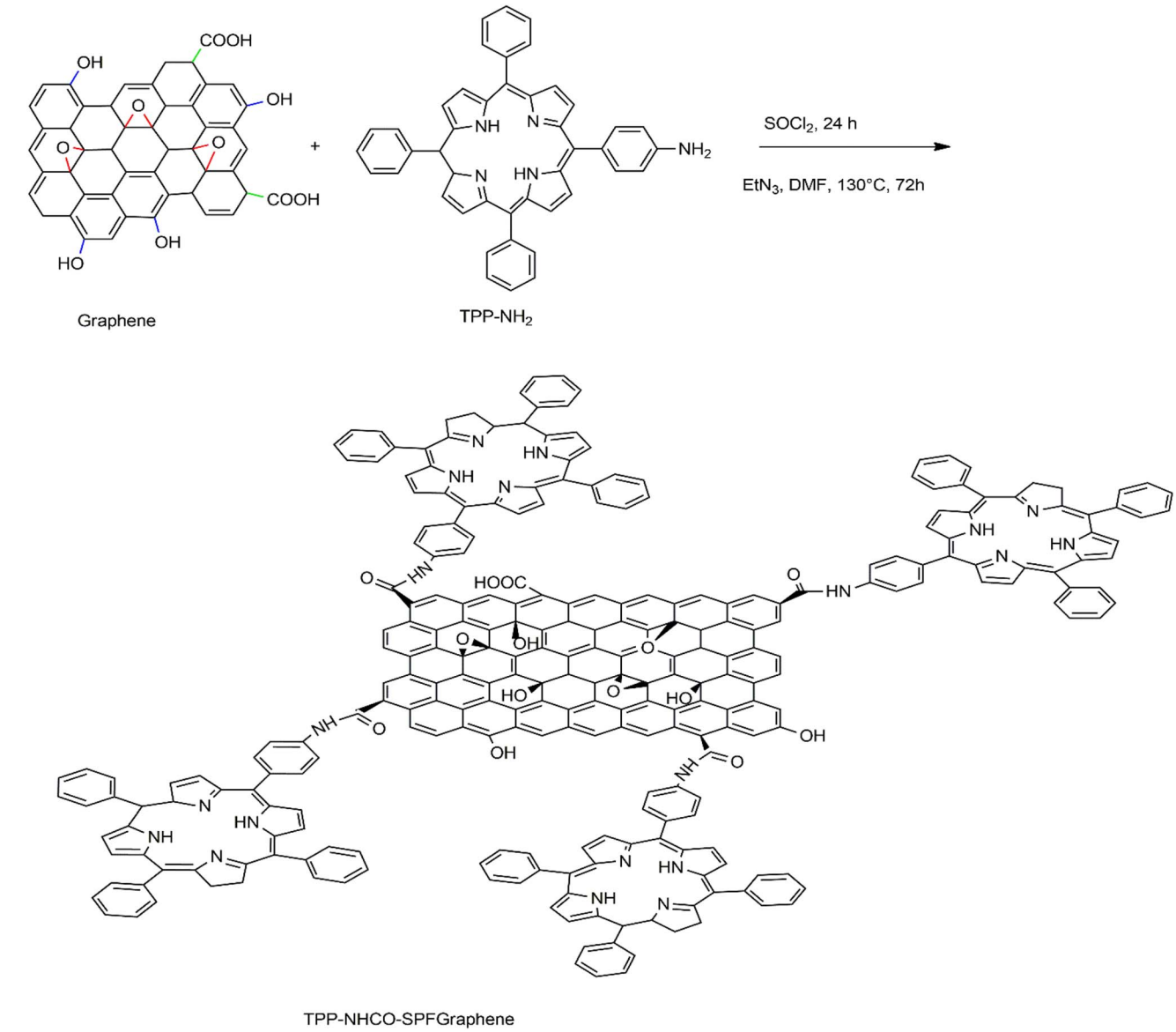

Fig. 21 Illustration of tetrephenylporphyrin (TPP) organic-solution-processable as the functionalization agent from graphene oxide in the presence of $SOCl_2$ over 24 hours.

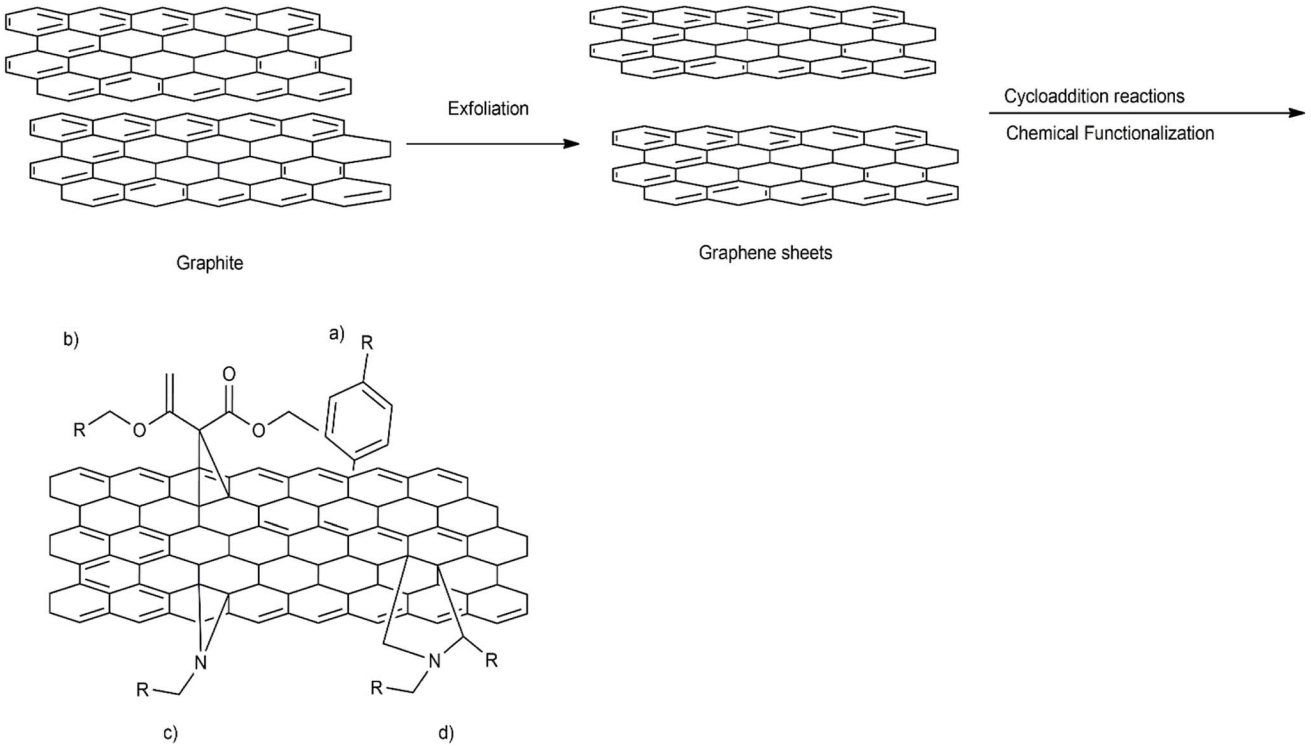

Fig. 22 Illustration of multi-functionalized product from exfoliated sheets of graphene through various cycloaddition reactions.

graphene composite in water. This makes it essential to functionalize cellulose with pyrene groups.[181] The polysaccharide is better at attaching onto graphene surfaces due to the π–π interactions, as illustrated in Fig. 18. Lotya *et al.*[179] reported a modified method to disperse graphite in surfactant–water solutions (SDBS/H_2O) through sonication, resulting in large-scale exfoliation, yielding large quantities of multilayered graphene. The exfoliated flakes are stabilized against re-aggregation by a relatively large potential barrier of the Coulomb's repulsion between surfactant-coated sheets (Fig. 19).

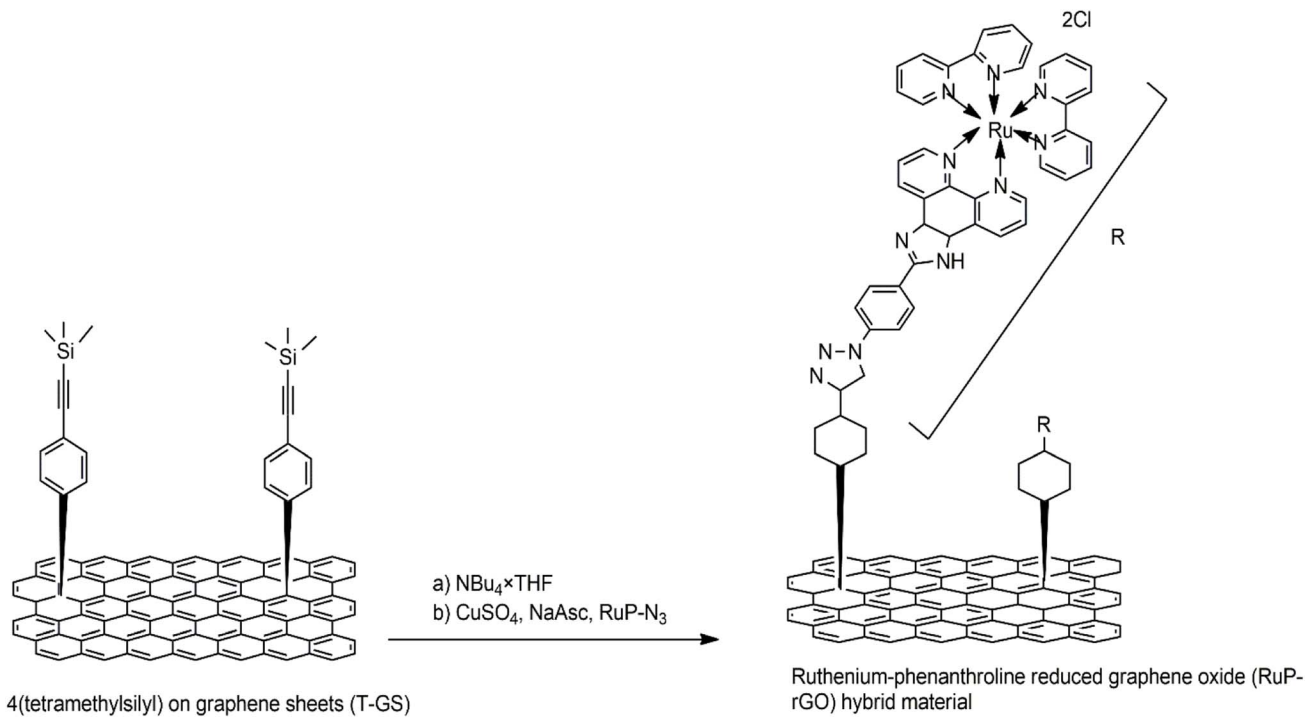

Fig. 23 Click reaction for the grafting of a porphyrin onto reduced graphene oxide sheets that were pre-modified by phenylacetylene units.

Bourlinos *et al.*[176] reported the treatment of crystalline graphite powder with an aqueous solution of PVP under sonication (Fig. 20), which resulted in a water-soluble polymer, protecting single-layer graphene without oxidation or destruction of the sp^2 character of the carbon core in graphene (2D; sp^2-hybridized crystal of carbon atom). The delocalized π-electrons can be formed with unpaired p-electrons, resulting in non-covalent interfacial interaction, established between graphene and polymer. This mainly involves a delocalized π-bond.[182] The exfoliation mechanism in such a type of polymer-assisted liquid exfoliation is discussed for different types of interfacial interaction, such as CH–π (Fig. 20(a)), π–π stacking (Fig. 20(b)) and cation–π (Fig. 20(c)).[183] This mechanism can be directly applied for the yield of high-quality graphenes coated with cellulose derivatives, chitosan, PVP, polyvinyl chloride (PVC), polyethylene (PE) and certain proteins like lignin, which can be directly applied for a high yield of graphene-coated nanomaterials.

4.2.4 Donor–acceptor hybrid materials. The use of donor–acceptor hybrid materials bonded onto a graphene structure

Table 3 Applications of graphene and graphene-based materials in various fields

Graphene/derivatives/ graphene based nanomaterials	Applications in various fields	References
Graphene	• Used as adsorbent in analytical sample preparation due to large surface area, π-electron rich surface and good thermal and chemical stability, used as solid phase extractor also.	189–192
	• Used as matrix in matrix-assisted laser desorption/ionization mass spectrometry.	193
	• Used for the encapsulation of metal or metal oxide nanoparticles, improving significantly the cycling performance of particles as anode in rechargeable Li metal batteries (RLBs).	194
	• Graphene-modified electrode is applied in selective determination of dopamine, eliminating ascorbic acid, its used as ink for 3D printing.	195
Graphene oxide	• Used as super capacitors.	196
	• Used as membranes, adsorbents, medicines, biology sensors for hydrogen, nitrogen, ultra-sensitive sensor for environmental monitoring.	197 and 198
	• Used as microwave absorbers for electromagnetic interference for environmental protection.	199
	• Used for the detection of nucleic acid, is done by tagging GO with fluorescent-labeled ssDNA.	200
Reduced graphene oxide	• Used as conductive transport coatings.	201
	• Used as electric interconnects on flexible substrates, organic light emitting devices (OLEDs), and active elements (field effect transistors).	202
	• Used in dye sensitized solar cells based on liquid electrolytes, photo-catalyst as binders, catalyst, and lithium batteries.	203 and 204
Graphyne	• Used as nanofilers, transistors, sensors, semiconductor metal hybrids, anisotropic conductors, and desalinators.	37
Graphdiyne	• Used as field effect transistors and sensors.	205 and 206
Graphone	• Used in inorganic ferroelectronics and molecular packing.	37
Graphane	• Hydrogen storage, biosensing, and spintronics.	207
Fluorogaphene	• Graphite fluoride (GrF) batteries, metal free catalyst for oxygen reduction reaction	30
	• Fabrication of sensor for ascorbic acid and uric acid, biosensor for NaDH and dopamine.	208
	• Used for solar cell production.	209
	• Used as metal free catalyst for oxygen reduction reactions.	210
	• Utilized as metal free contrast agent in magnetic resonance imaging.	211
	• Utilized for cellular imaging to display enhances in photostability at different pH values against singlet oxygen evolving during excitation.	30
Graphene based nanomaterials	• Used as receptors (antibody, single-stranded DNA,enzyme) combined with target ions, molecules, nucleic acid, photo-thermal therapy.	212
	• Used in bone tissue engineering.	213
	• Graphene based platinum is most widely used in oxygen reduction reaction as catalyst for fuel cells.	214
	• Hetero atom doped graphene prevent the loss of active sites by reducing dissolution of Ostwald ripening.	215
	• Helping to strengthen the bond between doped graphene and metal catalyst.	216
	• Nitrogen doped graphene potential substitute is used as catalyst for metals in alkaline condition thereby, improving the kinetics which is limited by intermediates formed in the two-electron pathways.	217
	• Boron doped graphene using spin-dopant method is used to provide an impurity source for semiconductor junction fabrication.	218
	• Used for water splitting.	219
	• Used as photocatalyst, CdS/GO is used as visible-light-absorbing photocatalyst.	220

facilitates the charge-transfer phenomenon. This is illustrated in Fig. 21, where porphyrins have been incorporated onto the graphene sheets.[184] Tetraphenylporphyrin (TPP) light-harvesting antennae have high excitation coefficients and show remarkable redox properties, making them promising electron donors when associated with graphene. Organic-solution-processable functionalized graphene (OSPF-Graphene), a hybrid material, was the first organic-solution-synthesized graphene. This material showed better optical limiting properties than benchmark materials. The process of chemical functionalization toward the formation of donor–acceptor hybrids performs the exfoliation of graphite with various cyclo-addition (CA) reactions. Fig. 22 reveals the (3 + 2) 1,3 dipolar CA of in-situ-generated azomethinylides to introduce fused pyrrolidine rings into the skeleton of graphene.[185,186] These organic 1,3 dipoles possess a carbanion which is next to an iminium ion. The product formed shows the addition of azomethinylides, fused pyrrolidine rings formed at the junction between two six-membered rings of the graphene lattice at site (a). This helps in the preparation of numerous custom-synthesized graphene-based materials. (1 + 2) CA of malonate derivatives, known as the Bingel reaction, yields cyclopropane rings on graphene. Carbon nucleophiles from alpha-halo esters and their subsequent region-selective addition to the graphene sheet are generated. The addition takes place on the double bonds between two six-membered rings present on graphene. This yields methano-modified graphene-based composites at site (b) in Fig. 22. Conversely, aryl diazonium salts proceeding *via* the release of dinitrogen, promote chemical functionalization towards the formation of donor–acceptor hybrids.[187] Here, an electron transfer from graphene to the diazonium salt results in the formation of an aryl unit, which gets added to the sp^2-carbon lattice of graphene at site (c). In addition to above-cited examples, the addition of azides results in the formation of azirdine adducts on hexagonal sheets, occurring *via* nitrines as a result of thermal decomposition of azides and thus, the release of dinitrogen takes place at site (d). In a nutshell, it has been observed that functionalization of graphene increases its solubility and enhances the processability of the material, which otherwise is insoluble, and so inapplicable for technological applications when stacked in the form of graphite. Furthermore, the preparation of novel nano-hybrid graphene materials is showing strong potential as they have promising applications in solar and photochemical cells. Such nanocomposites were formed using reduced graphene oxide that was initially modified by phenylacetylene units, used to mediate the grafting of ruthenium-phenanthroline (RuP) chromophores through a copper-catalyzed "click chemistry" reaction (Fig. 23).[188]

5 Potential applications of graphene and its derivatives

Graphene is a wonder material on Earth. Due to its high electric/thermal conductivity, mechanical strength and corrosion resistance, its potential application in high-power energy transmission has been well recognized. In future, it may replace the use of copper. Sensors, transparent electrodes, energy storage, coatings, electronics, biopolymer composites and biomedical device fabrications are some promising fields where graphene has a tremendous market. Industries based on energy storage and composites are going to make up most of the graphene market in the future. Graphene coatings are of tremendous significance in batteries, generators and conductors, leading to an improvement in energy efficiency and output. It might be a suitable replacement for indium-tin-oxide polymer-based solar cells in the near future. Its high surface area and biocompatibility make it one of the most attractive nanomaterials nowadays for drug/gene delivery, medical imaging, tissue engineering, photo-thermal therapy, biosensing and immunotherapy. Graphene, being lightweight, chemically inert and flexible, is one of the most sustainable materials. Currently, it has significant sustainable use in cellular imaging and cancer treatment in nano-biotechnological fields. Since bonding in graphene allows faster electron mobility, the development of transistors based on graphene has been a tremendous breakthrough. Thus, the replacement of the development of transistors built on silicon wafers is expected in a broad way in the near future. Smart solar panels in hydrogen fuel cell engineering is also a promising upcoming research field. However, recent significant applications of graphene, its derivatives and graphene-based nanocomposites are reported in detail in Table 3.[189–220]

6 Future perspectives and conclusions

Graphene, its derivatives and graphene-based nanocomposites are wonder nanomaterials of the future world. Graphene is the first ever artificial 2D carbon-based material that has potential affinity to transform energy-based industries to electronics. They have a wide variety of applications that will change the entire world in the future. Future graphene-material-based sensors will be designed to mimic human perception. Biocompatible devices, biomedicine, drug delivery, energy storage capacity, smart fuel cells/batteries and supercapacitors are some of its major promising applications. The biggest challenge in fact is the synthesis of pure graphene and its quantum yield. It definitely plays a crucial role in the target applications. The challenge lies in the defects, imperfections in the alignment of atoms, impurities, grain boundaries, multiple domains, structural disorders and wrinkles which are often observed in a graphene sheet that have an adverse effect on its optical, electrical, thermal and electronic properties. In electronic applications, the major bottleneck is the requirement for large-sized samples, which is possible to meet to a large extent by using a CVD process for its fabrication. However, it is difficult to produce high-quality and single-crystalline graphene and its subsequent thin films possessing very high electrical and thermal conductivities, along with excellent optical transparency. There is a considerable disadvantage and an issue of concern in the synthesis of graphene and its derivatives by

conventional methods, as it involves the usage of toxic chemicals. These methods usually result in the generation of hazardous waste and poisonous gases, leading to non-environmentally friendly issues. Therefore, Greener Technology being sustainable is coming up in a broad way. In fact, there is a need to develop a proper, sustainable green methodology to produce graphene and its various nano-derivatives and composites by following environmentally friendly approaches. Nevertheless, the controlled synthesis of doped graphene and its derivatives and controlled reduction and proper functionalization of graphene and its derivatives are highly warranted. The mechanisms involved in the reactions in many electrochemical and thermodynamic systems are still complicated. Additionally, thorough investigations must be made in the domain of doped graphene materials, which will have a tremendous impact on the green energy and semiconductor technology revolution in the future.

Conflicts of interest

There are no conflicts to declare.

Acknowledgements

The coauthor is grateful to the University Grant Commission and North Eastern Hill University, Shillong for providing, Non-Net Fellowship as financial assistance during the research programme.

References

1 E. Gerstner, Nobel Prize2010: Andre Geim and Konstantin Novoselov, *Nat. Phys.*, 2010, **6**(11), 836.
2 J. Wu, W. Pisula and K. Müllen, Graphenes as potential material for electronics, *Chem. Rev.*, 2007, **107**(3), 718–747.
3 H. Zhang, X. Lv, Y. Li, *et al.*, P25-graphene composite as a high performance photocatalyst, *ACS Nano*, 2009, **4**(1), 380–386.
4 H. Liu, S. Ryu, Z. Chen, *et al.*, Photochemical reactivity of graphene, *J. Am. Chem. Soc.*, 2009, **131**(47), 17099–17101.
5 X. Wang, L. Zhi and K. Müllen, Transparent, conductive graphene electrodes for dye- sensitized solar cells, *Nano Lett.*, 2008, **8**(1), 323–327.
6 G. Eda, Y. Y. Lin, S. Miller, *et al.*, Transparent and conducting electrodes for organic electronics from reduced graphene oxide, *Appl. Phys. Lett.*, 2008, **92**(23), 233305.
7 F. Schedin, A. Geim, K. Morozov, *et al.*, Detection of individual gas molecules adsorbed on graphene, *Nat. Mater.*, 2007, **6**(9), 652–655.
8 J. T. Robinson, F. K. Perkins, E. S. Snow, *et al.*, Reduced graphene oxide molecular Sensors, *Nano Lett.*, 2008, **8**(10), 3137–3140.
9 D. Fowler, M. J. Allen, V. Tung, *et al.*, Practical chemical sensors from chemically derived graphene, *ACS Nano*, 2009, **3**(2), 301–306.
10 K. S. Kim, Y. Zhao, H. Jang, *et al.*, Large-scale pattern growth of graphene films for stretchable transparent electrodes, *Nature*, 2009, **457**(7230), 706–710.
11 P. Blake, P. D. Brimicombe, R. R. Nair Booth, *et al.*, Graphene-based liquid crystal Device, *Nano Lett.*, 2008, **8**(6), 1704–1708.
12 Z. Guo, P. Zhang, J. Chetwynd, *et al.*, Elucidating the mechanism of the surface functionalization dependent neurotoxicity of graphene family nanomaterials, *Nanoscale*, 2020, **12**(36), 18600–18605.
13 S. Lian, Y. Qu, S. Li, *et al.*, Interaction of graphene-family nanomaterials with microbial communities in sequential batch reactors revealed by high-throughput sequencing, *Environ. Res.*, 2020, **184**, 109392.
14 M. Inagaki and F. Kang, Graphene derivatives: graphane, fluorographene, graphene oxide, graphyne and graphdiyne, *J. Mater. Chem. A*, 2014, **2**(33), 13193–13206.
15 S. Su, Q. Sun, X. Gu, *et al.*, Two-dimensional nanomaterials for biosensing applications, *TrAC, Trends Anal. Chem.*, 2019, **119**, 115610.
16 J. Wang, X. Jin, C. Li, *et al.*, Graphene and graphene derivatives toughening polymers: toward high toughness and strength, *Chem. Eng. J.*, 2019, **370**, 831–854.
17 T. M. Magne, T. de Oliveira Vieira, L. M. R. Alencar, *et al.*, Graphene and Its derivatives: understanding the main chemical and medicinal chemistry roles for biomedical applications, *J. Nanostruct. Chem.*, 2021, **12**, 693–727.
18 W. Yu, L. Sisi, Y. Haiyan, *et al.*, Progress in the functional modification of graphene/graphene oxide: a review, *RSC Adv.*, 2020, **10**(26), 15328–15345.
19 D. Sahu, H. Sutar, P. Senapati, *et al.*, Graphene, graphene–derivatives and composites: fundamentals, synthesis approaches to applications, *J. Compos. Sci.*, 2021, **5**(7), 181.
20 F. Catania, E. Marras, M. Giorcelli, *et al.*, A review on recent advancements of graphene and graphene-related materials in biological applications, *Appl. Sci.*, 2021, **11**(2), 614.
21 J. Sturala, J. Luxa, M. Pumera, *et al.*, Chemistry of graphene derivatives: synthesis, applications, and perspectives, *Chem. - Eur. J.*, 2018, **24**(23), 5992–6006.
22 A. N. Banerjee, Graphene and its derivatives as biomedical material: future prospects and challenges, *Interface Focus*, 2018, **8**(3), 20170056.
23 A. B. Ganganboina and R.-A. Doong, Nitrogen doped graphene quantum dot-decorated earth-abundant nanotubes for enhanced capacitive deionization, *Environ. Sci.: Nano*, 2020, **7**, 228–237.
24 Y. Gong, L. Shen, Z. Kang, *et al.*, Progress in energy-related graphyne- based materials: advanced synthesis, functional mechanisms and applications, *J. Mater. Chem. A*, 2020, **8**(41), 21408–21433.
25 Y. Zheng, Q. Feng, N. Tang, *et al.*, Synthesis and photoluminescence of graphdiyne, *New Carbon Mater.*, 2018, **33**(6), 516–521.
26 N. Narita, S. Nagagi, S. Suzuki, *et al.*, Optimized geometries and electronic structures of graphyne and its family, *Phys. Rev. B: Condens. Matter*, 1998, **58**(16), 11009–11014.

27 M. M. Haley, Synthesis and properties of annulenic subunits of graphyne and graphdiyne nano architectures, *Pure Appl. Chem.*, 2008, **80**(3), 519–532.
28 A. LIvanovskii, Graphynes and graphdyines, *Prog. Solid State Chem.*, 2013, (1), 1–19.
29 B. G. Kim and H. J. Choi, Graphyne: hexagonal network of carbon with versatile Dirac cones, *Phys. Rev. B: Condens. Matter Mater. Phys.*, 2012, **86**, 115435.
30 D. D. Chronopoulos, A. Bakandritsos, M. Pykal, *et al.*, Chemistry, properties, and applications of fluorographene, *Appl. Mater. Today*, 2017, **9**, 60–70.
31 R. R. Nair, W. Ren, R. Jalil, *et al.*, Fluorographene: a two-dimensional counterpart of teflon, *Small*, 2010, **6**, 2877–2884.
32 J. T. Robinson, J. S. Burgess and C. E. Junkermeier, Properties of fluorinated graphene films, *Nano Lett.*, 2010, **10**(8), 3001–3005.
33 L. Fengand and W. X. Zhang, The structure and magnetism of graphone, *AIP Adv.*, 2012, **2**(4), 042138.
34 S. H. Dave, C. Gong, A. W. Robertson, *et al.*, Chemistry and structure of graphene oxide via direct imaging, *ACS Nano*, 2016, **10**(8), 7515–7522.
35 M. Wojtoniszak, X. Chen, R. J. Kalenczuk, *et al.*, Synthesis, dispersion, and cytocompatibility of graphene oxide and reduced graphene oxide, *Colloids Surf., B*, 2012, **89**, 79–85.
36 J. Zhou, Q. Wang, Q. Sun, *et al.*, Ferromagnetism in semihydrogenated graphene sheet, *Nanolett*, 2009, **9**(11), 3867–3870.
37 Q. Peng, J. Crean, L. Han, *et al.*, New materials graphyne, graphdiyne, graphone, and graphane: review of properties, synthesis, and application in nanotechnology, *Nanotechnol., Sci. Appl.*, 2014, **7**, 1.
38 H. Li, R. Papadakis, T. Hussain, *et al.*, Moiré patterns arising from bilayer graphone/graphene superlattice, *Nano Res.*, 2020, **13**(4), 1060–1064.
39 S. Costamagna, M. Neek-Amal, J. H. Los, *et al.*, Thermal rippling behavior of graphane, *Phys. Rev. B: Condens. Matter Mater. Phys.*, 2012, **86**(4), 86041408.
40 S. Lebègue, M. K lintenberg, O. Eriksson, *et al.*, Accurate electronic band gap of pure and functionalized graphane from GW calculations, *Phys. Rev. B: Condens. Matter Mater. Phys.*, 2009, **79**(24), 245117.
41 H. Şahin, M. Topsakal and S. Ciraci, Structures of fluorinated graphene and their signatures, *Phys. Rev. B: Condens. Matter Mater. Phys.*, 2011, **83**(11), 205417.
42 D. C. Elias, R. R. Nair, T. M. G. Mohiuddin, *et al.*, control of graphene's properties by reversible hydrogenation: evidence for graphane, *Science*, 2009, **323**, 610.
43 L. Zhao, R. He, K. Rim, *et al.*, Visualizing individual nitrogen dopants in monolayer graphene, *Science*, 2011, **333**(6045), 999–1003.
44 H. Terrones, R. Lv, M. Terrones, *et al.*, The roleofdefectsanddopingin2Dgraphene sheets and 1D nanoribbons, *Rep. Prog. Phys.*, 2012, **75**(6), 062501.
45 M. Peralta, C. Vaca-Chanatasig, R. Vera-Nieto, *et al.*, Transport properties of graphene in proximity with alkali metals, *J. Phys.: Conf. Ser.*, 2022, **2238**(1), 012003.
46 M. Scardamaglia, H. Bluhm, H. Nemsak, *et al.*, Depth distribution of alkali metal ions on supported graphene in the presence of water, *J. Electron Spectrosc. Relat. Phenom.*, 2023, **262**, 147281.
47 F. Calleja, H. Ochoa, M. Garnica, *et al.*, Spatial variation of a giant spin–orbit effect induces electron confinement in graphene on Pb islands, *Nat. Phys.*, 2014, **11**, 43–47.
48 P. Rosenzweig, H. Karakachian, D. Marchenko, *et al.*, Overdoping graphene beyond the van hove singularity, *Phys. Rev. Lett.*, 2020, **125**, 176403.
49 K. V. Emtsev, A. A. Zakharov, C. Coletti, *et al.*, Ambipolar doping in quasi free epitaxial graphene on SiC(0001) controlled by Ge intercalation, *Phys. Rev. B: Condens. Matter Mater. Phys.*, 2011, **84**, 125423.
50 M. Sicot, P. Leicht, A. Zusan, *et al.*, Size-selected epitaxial nano islands underneath graphene Moir'e on Rh(111), *ACS Nano*, 2012, **6**, 151–158.
51 G. Profeta, M. Calandra and F. Mauri, Phonon-mediated superconductivity in graphene by lithium deposition, *Nat. Phys.*, 2012, **8**, 131–134.
52 M. Xue, G. Chen, H. Yang, *et al.*, Super conductivity in potassium-doped few-layer graphene, *J. Am. Chem. Soc.*, 2012, **134**, 6536–6539.
53 K. S. Novoselov, A. K. Geim, S. V. Morozov, *et al.*, Electric field effect in atomically thin carbon films, *Science*, 2004, **306**, 666–669.
54 L. Wang, J.-T. Ye, H.-Q. Wang, *et al.*, Third order nonlinear optical properties of endohedral fullerene (H2) 2@ C70 and (H2O) 2@ C70 accompanied by the prospective of novel (HF) 2@C70, *J. Phys. Chem. C*, 2018, **122**, 6835–6845.
55 J. Shi, H. Chu, Y. Li, *et al.*, Synthesis and nonlinear optical properties of semiconducting single-walled carbon nanotubes at 1 μm, *Nanoscale*, 2019, **11**, 7287–7292.
56 J. J. Tan and F. L. Gu, Tuning the nonlinear optical response of graphitic carbon nitride by doping Li atoms, *J. Phys. Chem. C*, 2018, **122**, 26635–26641.
57 S. Sarwar, J. Yaqoob, M. U. Khan, *et al.*, Deciphering the role of alkali metals (Li, Na, K) doping for triggering nonlinear optical (NLO) properties of t-graphene quantum dots: toward the development of giant NLO response materials, *ACS Omega*, 2022, **7**(28), 24396–24414.
58 A. K. Srivastava, Lithiated graphene quantum dot and its nonlinear optical properties modulated by a single alkali atom: a theoretical perspective, *Inorg. Chem.*, 2021, **60**, 3131–3138.
59 R. Nazir, J. Yaqoob, M. U. Khan, *et al.*, An effective strategy for tuning nonlinear optical response of N-atom functionalized corannulene by alkali metals doping: first theoretical insight, *Comput. Theor. Chem.*, 2021, **1205**, 113430.
60 O. Concepcion, A. Ali, M. F. Khalid, *et al.*, Facile Synthesis of diversely functionalized peptoids, spectroscopic characterization, and DFT-based nonlinear optical exploration, *ACS Omega*, 2021, **6**, 26016–26025.
61 K. Ayub, Are Phosphide Nano-Cages Better than Nitride Nano-Cages? A Kinetic, Thermodynamic and Non-Linear Optical Properties Study of Alkali Metal Encapsulated

X12Y12 Nano-Cages, *J. Mater. Chem. C*, 2016, **4**(46), 10919–10934.

62 F. A. Khazaal, M. M. Kadhim, H. F. Husseein, *et al.*, Electronic transfers and (nlo) properties predicted by ab initio methods with prove experimentally, *Neuroquantology*, 2020, **18**, 4654.

63 M. Khalid, M. U. Khan, I. Shafiq, *et al.*, NLO potential exploration for D–π–A hetero cyclic organic compounds by incorporation of various π-linkers and acceptor units, *Arab. J. Chem.*, 2021, **14**, 103295.

64 Y. Sharma, M. Mukhopadhyay, S. K. Pati, *et al.*, Linear and nonlinear optical properties of graphene quantum dots: a computational study, *J. Phys. Chem. C*, 2015, **119**(21), 1207912087.

65 H. Li, Z. Bi, R. Xu, *et al.*, Theoretical study on electronic polarizability and second hyperpolarizability of hexagonal graphene quantum dots: effects of size, substituent, and frequency, *Carbon*, 2017, **122**, 756–760.

66 D. Marchiani, A. Tonelli, C. Mariani, *et al.*, Tuning the electronic response of metallic graphene by potassium doping, *Nano Lett.*, 2022, **2**(1), 170–176.

67 Y. Wang, Y. Zheng, C. Han, *et al.*, Surface Charge Transfer Doping for Two-Dimensional Semiconductor-Based Electronic and Optoelectronic Devices, *Nano Res.*, 2021, **14**(6), 1682–1697.

68 L.-P. Ma, W. Ren and H.-M. Cheng, Progress in surface charge transfer doping of graphene, *Acta Phys.-Chim. Sin.*, 2022, **38**, 2012080.

69 C. Ataca, E. Aktürk and S. Ciraci, Hydrogen storage of calcium atoms adsorbed on graphene:first-principles plane wave calculations, *Phys. Rev. B: Condens. Matter Mater. Phys.*, 2009, **79**(4), 041406.

70 T. Hussain, B. Pathak, T. A. Maark, *et al.*, Ab initio study of lithium-doped graphane for hydrogen storage, *Europhys. Lett.*, 2011, **96**(2), 27013.

71 M. Khazaei, M. S. Bahramy, N. S. Venkataramanan, *et al.*, Chemical engineering of prehydrogenatedCandBN-sheetsbyLi:Applicationinhydrogenstorage, *J. Appl. Phys.*, 2009, **106**(9), 094303.

72 P. Chen, X. Wu, J. Lin, *et al.*, High H2 uptake by alkali-doped carbon nano tubes under ambient pressure and moderate temperatures, *Science*, 1999, **285**(5424), 91–93.

73 R. T. Yang, Hydrogen storage by alkali-doped carbon nanotubes–revisited, *Carbon*, 2000, **38**(4), 623–626.

74 F. E. Pinkerton, B. G. Wicke, C. H. Olk, *et al.*, Thermogravimetric measurement of hydrogen absorption in alkali-modified carbon materials, *J. Phys. Chem. B*, 2000, **104**(40), 9460–9467.

75 W.-Q. Deng, X. Xu and W. A. Goddard, New alkali doped pillared carbon materials designedtoachieve practicalreversiblehydrogenstoragefortransportation, *Phys. Rev. Lett.*, 2004, **92**(16), 166103.

76 I. Cabria, M. J. López and J. A. Alonso, Enhancement of hydrogen physisorption on graphene and carbon nanotubes by Li doping, *J. Chem. Phys.*, 2005, **123**(12), 204721.

77 W. Liu, Y. H. Zhao, Y. Li, *et al.*, Enhanced hydrogen storage on Li-dispersed carbon nanotubes, *J. Phys. Chem. C*, 2009, **113**(5), 2028–2033.

78 T. Hussain, B. Pathak, T. A. Maark, *et al.*, Functionalization of graphane with alkali and alkaline-earth metals: an insulator-to-metallic transition, *Europhys. Lett.*, 2012, **99**(4), 47004.

79 M. Drogeler, C. Franzen, F. Volmer, *et al.*, Spin life times exceeding12n sin graphene non local spin valve devices, *Nano Lett.*, 2016, **16**, 3533–3539.

80 A. Krasheninnikov, P. Lehtinen, A. Foster, *et al.*, Embedding transition-metal atoms in graphene: structure, bonding, and magnetism, *Phys. Rev. Lett.*, 2009, **102**, 126807.

81 P. C. Lin, R. Villarreal, S. Achilli, *et al.*, Doping graphene with substitutional Mn, *ACS Nano*, 2021, **15**(3), 5449–5458.

82 X. Wang, G. Sun, P. Routh, *et al.*, Heteroatom –doped graphene materials: synthesis, properties and applications, *Chem. Soc. Rev.*, 2014, **43**, 7067–7098.

83 Y. Lee, S. Lee, Y. Hwang, *et al.*, Modulating magnetic characteristics of Pt embedded graphene by gas adsorption (N2,O2,NO2,SO2), *Appl. Surf. Sci.*, 2014, **289**, 445–449.

84 J. Dai, J. Yuan and P. Giannozzi, Gas adsorption on graphene doped with B, N, Al, and S:a theoretical study, *Appl. Phys. Lett.*, 2009, **95**(23), 232105.

85 Z. M. Ao, J. Yang, S. Li, *et al.*, Enhancement of CO detection in Al doped graphene, *Chem. Phys. Lett.*, 2008, **461**(4–6), 276–279.

86 P. A. Denis, Band gap opening of monolayer and bilayer graphene doped with aluminium, silicon,phosphorus, and sulfur, *Chem. Phys. Lett.*, 2010, **492**(4–6), 251–257.

87 Y. Zou, F. Li, Z. Zhu, *et al.*, An ab initio study on gas sensing properties of graphene and Sidoped graphene, *Eur. Phys. J. B*, 2011, **81**(4), 475–479.

88 Y. Chen, X. Yang, Y. Liu, *et al.*, Can Si-doped graphene activate or dissociate O2 molecule?, *J. Mol. Graph*, 2013, **39**, 126–132.

89 H.-M. Wang, H.-X. Wang, Y. Chen, *et al.*, Phosphorus-doped graphene and (8, 0) carbon nanotube: structural, electronic, magnetic properties, and chemical reactivity, *Appl. Surf. Sci.*, 2013, **273**, 302–309.

90 J. Dai and J. Yuan, Modulating the electronic and magnetic structures of P-doped graphene by molecule doping, *J. Condens. Matter Phys.*, 2010, **22**(22), 225501.

91 P. A. Denis, R. Faccio and A. W. Mombru, Is it possible to dope single-walled carbon nanotubes and graphene with sulfur?, *ChemPhysChem*, 2009, **10**(4), 715–722.

92 K. A. Mkhoyan, A. W. Contryman, J. Silcox, *et al.*, Atomic and electronic structure of graphene- oxide, *Nano Lett.*, 2009, **9**(3), 1058–1063.

93 D. W. Boukhvalov and M. I. Katsnelson, Modeling of graphite oxide, *J. Am. Chem. Soc.*, 2008, **130**(32), 10697–10701.

94 R. Zbořil, F. Karlický and A. B. Bourlinos, Graphene Fluoride: A stable stoichiometric graphene derivative and its chemical conversion to graphene, *Small*, 2010, **6**(24), 2885–2891.

95 M. A. Ribas, A. K. Singh, P. B. Sorokin, *et al.*, Patterning nano rods and quantum dots on fluorinated graphene, *Nano Res.*, 2010, **4**(1), 143–152.
96 H. Chang, J. Cheng, X. Liu, *et al.*, Synthesis of wide-band gap fluorinated graphene semiconductors, *Chem.–Eur. J.*, 2011, **17**(32), 8896–8903.
97 K.-J. Jeon, Z. Lee, E. Pollak, *et al.*, Fluorographene: A wide band gap semiconductor with ultraviolet luminescence, *ACS Nano*, 2011, **5**(2), 1042–1046.
98 B. Shen, J. Chen, X. Yan, *et al.*, Synthesis of fluorine-doped multi-layered graphene sheets by arc- discharge, *RSC Adv.*, 2012, **2**(17), 6761.
99 J. Wu, L. Xie, Y. Li, *et al.*, Controlled chlorine plasma reaction for non invasive graphene doping, *J. Am. Chem. Soc.*, 2011, **133**(49), 19668–19671.
100 B. Li, L. Zhou, D. Wu, *et al.*, Photochemical chlorination of graphene, *ACS Nano*, 2011, **5**(7), 5957–5961.
101 M. Yang, L. Zhou, J. Wang, *et al.*, Evolutionary chlorination of graphene: from charge-transfer complex to covalent bonding and nonbonding, *J. Phys. Chem. A*, 2011, **116**(1), 844–850.
102 P. V. C. Medeiros, A. J. Mascarenhas, F. D. Mota, *et al.*, A DFT study of halogen atoms adsorbed on graphene layers, *Nanotechnol*, 2010, **21**(48), 485701.
103 G. Kalita, K. Wakita, M. Takahashi, *et al.*, Iodine doping in solid precursor-based CVD growth graphene film, *J. Mater. Chem.*, 2011, **21**(39), 15209.
104 Z. Yao, H. Nie, Z. Yang, *et al.*, Catalyst-free synthesis of iodine-doped graphene via a facile thermal annealing process and its use for electrocatalytic oxygen reduction in an alkaline medium, *Chem. Commun.*, 2012, **48**(7), 1027–1029.
105 L. Ci, L. Song, C. Jin, *et al.*, Atomic layers of hybridized boron nitride and graphene domains, *Nat. Mater.*, 2010, **9**(5), 430–435.
106 H. Nozaki and S. Itoh, Structural stability of B2CN, *J. Phys. Chem. Solids*, 1996, **57**(1), 41–49.
107 S. Bhandary and B. Sanyal, in *Composite and their Properties*, ed. N. Hu, InTechOpen, London, 2012, ch. 1, pp. 3–16.
108 P. Rani and V. K. Jindal, Stability and electronic properties of isomers of B/N Co-doped graphene, *Appl. Nanosci.*, 2013, **4**(8), 989–996.
109 B. Muchharla, A. Pathak, Z. Liu, *et al.*, Tunable electronics in large-area atomic layers of Boron–nitrogen–carbon, *Nano Lett.*, 2013, **13**(8), 3476–3481.
110 H. Tachikawa, T. Iyama, K. T. Azumi, *et al.*, Density functional theory study of boron-and nitrogen-atom-doped graphene chips, *Jpn. J. Appl. Phys.*, 2011, **50**, 01BJ03.
111 Y. Xue, D. Yu, L. Dai, *et al.*, Three- dimensional B, N-doped graphene foam as a metal- free catalyst for oxygen reduction reaction, *Phys Chem Chem Phys*, 2013, **15**(29), 12220–12226.
112 J. B. Matsoso, C. Journet, N. J. Coville, *et al.*, Co-doping graphene with B and N heteroatom for application in energy conversion and storage devices, *ChemNanoMat*, 2022, **8**(7), 3–21.
113 Y. Dai, J. Ding, J. Li, *et al.*, N, S and Transition –metal Co-doped graphen nano composites as high-performance catalyst for glucose oxidation in a direct glucose alkaline fuel cell, *Nanomater*, 2021, **11**(1), 202.
114 S. Wang, L. Zhang, Z. Xia, *et al.*, BCN Graphene as Efficient Metal-Free Electrocatalyst for the Oxygen Reduction Reaction, *Angew. Chem., Int. Ed.*, 2012, **51**(17), 4209–4212.
115 Y. Dong, Y. Wu, M. Liu, *et al.*, Electrocatalysis on Shape-Controlled Titanium Nitride Nanocrystals for the Oxygen Reduction Reaction, *ChemSusChem*, 2013, **6**(10), 2016–2021.
116 C. H. Choi, M. W. Chung, H. C. Kwon, *et al.*, N- and P, N-Doped Graphene as Highly Active Catalysts for Oxygen Reduction Reactions in Acidic Media, *J. Mater. Chem. A*, 2013, **1**(11), 3694.
117 Y. Irmawati, F. Balqis, P. B. Persada, *et al.*, Iron-decorated nitrogen/boron Co-doped reduced graphene oxide aerogel for neutral rechargeable Zn-Air batteries, *Batteries*, 2023, **9**(7), 356.
118 N. H. Md. Said, W. W. Liu, C. S. Khe, *et al.*, Review of the past and recent developments in functionalization of graphene derivatives for reinforcement of polypropylene nanocomposites, *Polym. Compos.*, 2021, **42**(3), 1075–1108.
119 L. Peng, Z. Xu, Z. Liu, *et al.*, An iron-based green approach to1-H production of single- layer graphene oxide, *Nat. Commun.*, 2015, **6**, 5716.
120 S. Eigler and A. Hirsch, Chemistry with graphene and graphene oxide- challenges for synthetic chemists, *Angew. Chem., Int. Ed.*, 2014, **53**(30), 7720–7738.
121 L. D. David, V. Mercedes, S. Maria, *et al.*, The Role of oxidative debris on graphene oxide films, *ChemPhysChem*, 2013, **14**(17), 4002–4009.
122 D. C. Marcano, D. V. Kosynkin, J. M. Berlin, *et al.*, Improved synthesis of graphene oxide, *ACS Nano*, 2010, **4**(8), 4806–4814.
123 W. S. Hummers and R. E. Offeman, Preparation of graphitic oxide, *J. Am. Chem. Soc.*, 1958, **80**, 1339.
124 J. T. Robinson, J. S. Burgess, C. E. Junermeier, *et al.*, Properties of fluorinated graphene films, *Nano Lett.*, 2010, **10**(8), 3001–3005.
125 X. Hong, S. H. Cheng, C. Herding, *et al.*, Colossal negative magneto resistance in dilute fluorinated graphene, *Phys. Rev. B: Condens. Matter Mater. Phys.*, 2011, **83**(8), 085410.
126 P. Gong, Z. Wang, J. Wang, *et al.*, One-pot sonochemical preparation of fluorographene and selective tuning of its fluorine coverage, *J. Mater. Chem.*, 2012, **22**(33), 16950.
127 Z. Wang, J. Wang, Z. Li, *et al.*, Synthesis of fluorinated graphene with tunable degree of fluorination, *Carbon*, 2012, **50**(15), 5403–5410.
128 F. Diederich, Carbon scaffolding: building acetylenic all-carbon and carbon-rich compounds, *Nature*, 1994, **369**(6477), 199–207.
129 C. Lee, X. Wei, J. W. Kysar, *et al.*, Measurement of the elastic properties and intrinsic strength of monolayer graphene, *Science*, 2008, **321**, 385–388.

130 G. Li, Y. Li, X. Qian, *et al.*, Construction of tubular molecule aggregations of graphdiyne for highly efficient field emission, *J. Phys. Chem. C*, 2011, **115**(6), 2611–2615.
131 Y. Yan, F. Nashath, Z. Chen, *et al.*, Synthesis of graphene: potential carbon precursors and approaches, *Nanotechnol. Rev.*, 2020, **9**, 1284–1314.
132 R. Paupitz, P. A. S. Autreto and S. B. Legoas, Graphene to fluoro graphene and fluorographane: a theoretical study, *Nanotechnol*, 2012, **24**(3), 035706.
133 P. Blake, E. W. Hill, A. H. Castro Neto, *et al.*, Making graphene visible, *Appl. Phys. Lett.*, 2007, **91**(6), 063124.
134 K. V. Emtsev, A. Bostwick, K. Horn, *et al.*, Towards wafer-size graphene layers by atmospheric pressure graphitization of silicon carbide, *Nat. Mater.*, 2009, **8**(3), 203–207.
135 B. Butz, C. Dolle, F. Niekiel, *et al.*, Dislocations in bilayer graphene, *Nature*, 2013, **505**(7484), 533–537.
136 A. M. Ilyin, N. R. Guseinov, I. A. Tsyganov, *et al.*, Computer simulation and experimental study of graphane-like structures formed by electrolytic hydrogenation, *Phys. E*, 2011, **43**(6), 1262–1265.
137 H. L. Poh, Z. Sofer and M. Pumera, Graphane electrochemistry: electron transfer at hydrogenated graphenes, *Electrochem. Commun.*, 2012, **25**, 58–61.
138 A. V. Talyzin, S. Luzan, I. V. Anoshkin, *et al.*, Hydrogenation, purification and unzipping of carbon nanotubes by reaction with molecular hydrogen: road to graphane nanoribbons, *ACS Nano*, 2011, **5**(6), 5132–5140.
139 N. Mishra, J. Boeckl, N. Motta, *et al.*, Graphene growth on silicon carbide: a review, *Phys. Status Solidi A*, 2016, **213**(9), 2277–2289.
140 J. R. Hajrus, L. C. Shriver-Lake, S. N. Dean, *et al.*, Modifications of epitaxial graphene on SiC for the electrochemical detection and identification of heavy metal salts in seawater, *Sensors*, 2022, **22**(14), 5367.
141 I. Sengupta, S. Chakraborty, M. Talukdar, *et al.*, Thermal reduction of graphene oxide: how temperature influences purity, *J. Mater. Res.*, 2018, **33**(23), 4113–4122.
142 R. M. Nauman Javed, A. Al-Othman, M. Twalbeh, *et al.*, Recent developments in graphene and graphene oxide materials for polymer electrolyte membrane fuel cells applications, *Renewable Sustainable Energy Rev.*, 2022, **168**, 112836.
143 G. S. Kumble, *Graphene oxide: applications and opportunities*, IntechOpen, London, 2018, vol. 160.
144 F. K. Alosaimi, T. T. Tung, V.-D. Dao, *et al.*, Graphene-based multi functional surface and structure gradients engineered by atmospheric plasma, *Appl. Mater. Today*, 2022, **27**, 101486.
145 M. Devi, S. Rawat and S. Sharma, A comprehensive review of the pyrolysis process: from carbon nanomaterial synthesis to waste treatment, *Oxf. Open Mater. Sci.*, 2020, **1**(1), 2633–6979.
146 M. Saeed, Y. Alshammari, S. A. Majeed, *et al.*, Chemical vapour deposition of graphene—Synthesis, characterization, and applications: A review, *Molecules*, 2020, **25**(17), 3856.
147 Y. Xu, H. Cao, Y. Xue, *et al.*, Liquid-phase exfoliation of graphene: an over view on exfoliation media, techniques, and challenges, *Nanomater*, 2018, **8**(11), 942.
148 C. Hu, Y. Shin, O. Read, *et al.*, Dispersant–Assisted Liquid–Phase Exfoliation of 2D Materials beyond Graphene, *Nanoscale*, 2020, **13**, 460–484.
149 B. H. Al-Tamimi, S. B. H. Farid and F. A. Chyad, Modified unzipping technique to prepare graphene nano-sheets, *J. Phys. Conf. Ser.*, 2018, **1003**(1), 012020.
150 A. Santhiram, P. Iyngaran, P. Abiman, *et al.*, Graphene synthesis and its recent advances in applications a review, *C*, 2021, **7**(4), 76.
151 D. A. Fendarkar, S. R. Thakare, S. M. Ramtekevet, *et al.*, Modification and functionalization of graphene/graphene oxide, *Methods*, 2015, **12**, 13.
152 M. Namvari, C. S. Biswas, Q. Wang, *et al.*, Crosslinking hydroxylated reduced graphene oxide with RAFT-CTA :a nano-initiator for preparation of well-defined amino acid-based polymer nanohybrids, *J. Colloid Interface Sci.*, 2017, **504**, 731–740.
153 K. C. Mei, N. Rubio, P. M. Costa, *et al.*, Synthesis of double-clickable functionalized graphene oxide for biological applications, *Chem. Comm.*, 2015, **51**(81), 14981–14984.
154 Z. Spitalsky, M. Danko, J. Mosnacek, *et al.*, Preparation of functionalized graphene sheets, *Curr. Org. Chem.*, 2011, **15**(8), 1133–1150.
155 A. K. Farquhar, H. M. Dykstra, M. R. Waterland, *et al.*, The spontaneous modification of free-floating few-layer graphene by aryldiazonium ions: electrochemistry, AFM and infrared spectroscopy from grafted films, *J. Phys. Chem. C*, 2011, **120**(14), 7543.
156 N. Mohanty and V. Berry, Graphene-based single-bacterium resolution bio-device and DNA transistor: interfacing graphene derivatives with nanoscale and micro scale biocomponents, *Nano Lett.*, 2008, **8**(12), 4469–4476.
157 Y. Cao, Z. Lai, J. Feng, *et al.*, Graphene oxide sheets covalently functionalized with block copolymers via click chemistry as reinforcing fillers, *J. Mater. Chem.*, 2011, **21**(25), 9271.
158 Z. Liu, J. T. Robinson, X. Sun, *et al.*, PEGylated Nano-Graphene Oxide for delivery of water insoluble cancer drugs, *J. Am. Chem. Soc.*, 2008, **130**(33), 10876–10877.
159 C. N. R. Rao and R. Voggu, Charge-transfer with graphene and nanotubes, *Mater. Today*, 2010, **13**(9), 34–40.
160 A. Ghosh, K. V. Rao, R. Voggu, *et al.*, Non-covalent functionalization, solubilization of graphene and single-walled carbon nanotubes with aromatic donor and acceptor molecules, *Chem. Phys. Lett.*, 2010, **488**(4–6), 198–201.
161 K. S. Subrahmanyam, R. Voggu, A. Govindaraj, *et al.*, A comparative raman study of the interaction of electron donor and acceptor molecules with graphene prepared by different methods, *Chem. Phys. Lett.*, 2009, **472**(1–3), 96–98.
162 T.-X. Ye, S.-l. Ye, D.-M. Chen, *et al.*, Spectroscopic characterization of tetra cationic porphyrins and their non covalent functionalization with graphene, *Spectrochim. Acta, Part A*, 2012, **86**, 467–471.

163 E. C. Lee, D. Kim, P. Jurecka, *et al.*, Understanding of assembly phenomena by aromatic- aromatic interactions: benzene dimer and the substituted systems, *J. Phys. Chem. A*, 2007, **111**, 3446–3457.

164 Q. Su, S. Pang, V. Alijani, *et al.*, Composites of graphene with large aromatic molecules, *Adv. Mater.*, 2009, **21**, 3191–3195.

165 X.-F. Zhang, S. P. Liu, X. N. Shao, *et al.*, Non covalent binding of xanthene and phthalocyanine dyes with graphene sheets: the effect of the molecular structure revealed by a photophysical study, *Spectrochim. Acta, Part A*, 2013, **113**, 92–99.

166 V. Georgakilas, J. N. Tiwari, K. C. Kemp, *et al.*, Non covalent functionalization of graphene and graphene oxide for energy materials, biosensing, catalytic, and biomedical applications, *Chem. Rev.*, 2016, **116**(9), 5464–5519.

167 J. S. Chia, M. T. T. Tan, P. S. Khiew, *et al.*, A bio-electrochemical sensing platform for glucose based on irreversible, non-covalent pi–pi functionalization of graphene produced via a novel, green synthesis method, *Sens. Actuators, B*, 2015, **210**, 558–565.

168 Y. Zhang, H. Li, Q. Wu, *et al.*, Non-covalent functionalization of graphene sheets by pyreneendcapped tetraphenylethene: enhanced aggregation-induced emission effect and application in explosive detection, *Front. Chem.*, 2022, **10**, 970033.

169 E. Y. Choi, T. H. Han, J. Hong, *et al.*, Non covalent functionalization of graphene with end functional polymers, *J. Mater. Chem.*, 2010, **20**, 1907–1912.

170 X. Ge, H. Li, L. Wu, *et al.*, Improved mechanical and barrier properties of starch film with reduced graphene oxide modified by SDBS, *J. Appl. Polym. Sci.*, 2017, **134**(22), 25.

171 H.-X. Wang and H.-L. Zhang, in *Graphene-New trends and devcelopments*, ed. F. Ebrahimi, InTechOpen, London, 2015, ch. 4, pp. 91–110.

172 Y. Wang, L. Sisi, H. Yang, *et al.*, Progress in the functional modification of graphene/graphene oxide: A review, *RSC Adv.*, 2020, **10**(26), 15328–15345.

173 P. Bhunia, H. Eunhee, M. Misook, *et al.*, Anon-volatile memory device consisting of graphene oxide covalently functionalized with ionic liquid, *Chem. Commun.*, 2012, **46**(6), 913–915.

174 M. J. Fernández-Merino, J. M. Paredes, S. Villar-Rodil, *et al.*, Investigating the influence of surfactants on the stabilization of aqueous reduced graphene oxide dispersions and the characteristics of their composite films, *Carbon*, 2012, **50**(9), 3184–3194.

175 Y. Hu, C. Neumann, L. Scholtz, *et al.*, Polarity intramolecular charge transfer, and hydrogen bond co-mediated solvent effects on the optical properties of graphene quantum dots, *Nano Res.*, 2022, **16**(1), 45–52.

176 A. B. Bourlinos, V. Georgakilas, R. Zboril, *et al.*, Aqueous-phase exfoliation of graphite in the presence of polyvinylpyrrolidone for the production of water-soluble graphenes, *Solid State Commun.*, 2009, **149**, 2172–2176.

177 Y. Liang, D. Wu, X. Feng, *et al.*, Dispersion of graphene sheets inorganic solvent supported by ionic interactions, *Adv. Mater.*, 2009, **21**, 1–5.

178 P. M. Carrasco, S. Montes, I. Garcia, *et al.*, High-concentration aqueous dispersions of graphene produced by exfoliation of graphite using cellulose nanocrystals, *Carbon*, 2014, **70**, 157–163.

179 M. Lotya, Y. Hernandez, P. J. King, *et al.*, Liquid phase production of graphene by exfoliation of graphite in surfactant/water solutions, *J. Am. Chem. Soc.*, 2009, **131**, 3611–3620.

180 M. Lotya, P. J. King, U. Khan, *et al.*, High-concentration, surfactant-stabilized graphene dispersions, *ACS Nano*, 2010, **4**(6), 3155–3162.

181 Q. Yang, X. Pan, F. Huang, *et al.*, Fabrication of high concentration and stable aqueous suspensions of graphene nanosheets by noncovalent functionalization with lignin and cellulose derivatives, *J. Phys. Chem. C*, 2010, **114**, 3811–3816.

182 J. Hwang, P. Li, M. D. Smith, *et al.*, Tipping the balance between S–π and O–π interactions, *J. Am. Chem. Soc.*, 2018, **140**, 13301–13307.

183 X. Han, J. Gao, T. Chen, *et al.*, Interfacial interaction and steric repulsion in polymer- assisted liquid exfoliation to produce high-quality graphene, *Chem. Pap.*, 2020, **74**(3), 757–765.

184 Y. Xu, Z. Liu, X. Zhang, *et al.*, A graphene hybrid material covalently functionalized with porphyrin: synthesis and optical limiting property, *Adv. Mater.*, 2009, **21**(12), 1275–1279.

185 M. Quintana, K. Spyrou, M. Grzelczak, *et al.*, Functionalization of graphene via1,3-dipolar cycloadddition, *ACS Nano*, 2010, **4**(6), 3527–3533.

186 A. Stergiou, G. Pagona and N. Tagmatarchis, Donor–acceptor graphene-based hybrid materials facilitating photo-induced electron-transfer reactions, *Beilstein J. Nanotechnol.*, 2014, **5**, 1580–1589.

187 E. Bekyarova, M. E. Itakis, P. Ramesh, *et al.*, Chemical modification of epitaxial graphene: spontaneous grafting of aryl groups, *J. Am. Chem. Soc.*, 2009, **131**(4), 1336–1337.

188 H.-X. Wang, K.-G. Zhou, Y.-L. Xie, *et al.*, Photo active graphene sheets prepared by click chemistry, *Chem. Commun.*, 2011, **47**(20), 5747.

189 Q. Liu, J. Shiand and G. Jiang, Application of graphene in analytical sample preparation, *TrAC, Trends Anal. Chem.*, 2012, **37**, 1–11.

190 W. Jing, J. Wang, B. Kuipers, *et al.*, Recent applications of graphene and graphene-based materials as sorbents in trace analysis, *TrAC, Trends Anal. Chem.*, 2021, **137**, 116212.

191 F. Pena-Pereira, V. Romero, I. dela Calle, *et al.*, Graphene–based nano composites in analytical extraction processes, *TrAC, Trends Anal. Chem.*, 2021, **142**, 116303.

192 E. V. S. Maciel, K. Mejía-Carmona, M. Jordan-Sinisterra, *et al.*, The current role of graphene-based nano materials in the sample preparation arena, *Front. Chem.*, 2020, **8**, 00664.

193 H. Liu, Y. Pan, C. Xiong, *et al.*, Matrix-assisted laser desorption/ionization mass spectrometry imaging (MALDI MSI) for in Situ analysis of endogenous small molecules in biological samples, *TrAC, Trends Anal. Chem.*, 2022, **157**, 116809.

194 K. Ullah, N. Shah, R. Wadood, *et al.*, Recent trends in graphene based transition metal oxides as anode materials for rechargeable lithium-ion batteries, *Nano Trends*, 2023, **1**, 100004.

195 A. Nag, R. B. V. Simorangkir, D. R. Gawade, *et al.*, Graphene-based wearable temperature sensors: a review, *Mater. Des.*, 2022, **221**, 110971.

196 A. T. Lawal, *et al.*, Graphene-based nano composites and their applications, a review, *Biosens. Bioelectron.*, 2019, **141**, 111384.

197 A. T. Dideikin and A. Y. Vul, Graphene oxide and derivatives : the place in graphene family, *Front. Phys.*, 2019, **6**, 149.

198 Q. U. A. Zahra, X. Fang, Z. Luo, *et al.*, Graphene based nano hybrid apta sensors in environmental monitoring: concepts, design and future outlook, *Crit. Rev. Anal. Chem.*, 2022, 1–22.

199 H. Zhang, N. Luo, T. Liu, *et al.*, Light-weight, low-loading and large-sheet reduced graphene oxide for high-efficiency micro wave absorber, *Carbon*, 2022, **196**, 1024–1034.

200 F. Pu, J. Ren, X. Qu, *et al.*, Recent progress in sensor arrays using nucleic acid as sensing elements, *Coord. Chem. Rev.*, 2022, **456**, 214379.

201 Y. Shi, M. Zhang, L. Zhang, *et al.*, Graphene oxide coated manganese dioxide electrode prepared by polyvinylpyrrolidone assisted electrodeposition, *Vacuum*, 2022, **199**, 110925.

202 H. Zhou, S. J. Han, A. K. Harit, *et al.*, Graphene-based intrinsically stretchable 2D- contact electrodes for highly efficient organic light-emitting diodes, *Adv. Mater.*, 2022, **34**(31), 2203040.

203 D. Suand and G. Centi, A perspective on carbon materials for future energy applications, *J. Energy Chem.*, 2013, **22**(2), 151–173.

204 S. Singh, Md. R. Hasan, P. Sharma, *et al.*, Graphene nanomaterials: The wondering material from synthesis to applications, *Sens. Int.*, 2022, **3**, 100190.

205 Z. Ghafary, A. Salimi, R. Hallaj, *et al.*, Exploring the Role of 2D-Graphdiyne as a Charge Carrier Layer in Field-Effect Transistors for non-covalent biological immobilization against human diseases, *ACS Biomater. Sci. Eng.*, 2022, **8**(9), 3986–4001.

206 J. Li, C. Wan, C. Wang, *et al.*, 2D material chemistry: Graphdiyne-basedbiochemical sensing, *Chem. Res. Chin. Univ.*, 2020, **36**(4), 622–630.

207 M. R. Rezapour, C. W. Myung, J. Yun, *et al.*, Graphene and graphene analogs toward optical,electronic,spintronic,green-chemical,energy-material,sensing,andmedical applications, *ACS Appl. Mater. Interfaces*, 2017, **9**(29), 24393–24406.

208 V. Urbanová, F. Karlický, A. Matěj, *et al.*, Fluorinated graphenes as advanced biosensors – effect of fluorine coverage on electron transfer properties and adsorption of biomolecules, *Chem. Sci.*, 2016, **8**(24), 12134–12142.

209 S. Javaid, M. Chang Woo, P. Saeed, *et al.*, A highly hydrophobic fluorographene-based system as an interlayer for electron transport in organic–inorganic perovskite solar cells, *J. Mater. Chem. A*, 2018, **6**(38), 18635–18640.

210 S. Zeng, S. Wang, H. Zhuang, *et al.*, Fluorine-doped carbon: A metal-free electrocatalyst for oxygen reduction to peroxide, *Electrochim. Acta*, 2022, **420**, 140460.

211 S. Radhakrishnan, A. Samanta, P. Sudeep, *et al.*, Metal-free dual modal contrast agents based on fluorographene quantum dots, *Part. Part. Syst. Charact.*, 2017, **34**(1), 1600221.

212 S. Han, J. Sun, M. Tang, *et al.*, The application of graphene-based bio materials in biomedicine, *Am. J. Transl. Res.*, 2019, **11**(6), 3246–3260.

213 Z. Du, C. Wang, R. Zhang, *et al.*, Applications of graphene and its derivatives in bone repair: advantages for promoting bone formation and providing real-time detection, challenges and future prospects, *Int. J. Nanomed.*, 2020, **15**, 7523–7551.

214 H. Suand and Y. Hu, Recent advances in graphene-based materials for fuel cell applications, *Energy Sci. Eng.*, 2020, **9**, 958–983.

215 Y. Yan, S. Woo In, H. Lee, *et al.*, A recent trend: application of graphene in catalysis, *Carbon Lett.*, 2021, **31**(2), 177–199.

216 M. Hu, Z. Yao, X. Wang, *et al.*, Graphene-based nanomaterials for catalysis, *Ind. Eng. Chem. Res.*, 2017, **56**(13), 3477–3502.

217 L. Qu, Y. Liu, J. Baek, *et al.*, Nitrogen-doped graphene as efficient metal-free electrocatalyst for oxygen reduction in fuel cells, *ACS Nano*, 2010, **4**(3), 1321–1326.

218 L. C. T. Cao, L. Hakim, *et al.*, *Boron Doping in Next-Generation Materials for Semiconductordevice, Characteristics and Applications of Boron*, IntechOpen, 2022.

219 G. Xie, K. Zhang, B. Guo, *et al.*, Graphene-based materials for hydrogen generation from light-driven water splitting, *Adv. Mater.*, 2013, **25**(28), 3820–3839.

220 N. Zhang, M.-Q. Yang, Z.-R. Tang, *et al.*, CdS–graphene nano composites as visible light photocatalyst for redox reactions in water: A green route for selective transformation and environmental remediation, *J. Catal.*, 2013, **303**, 60–69.